



Observational  
evidence for within  
canopy removal of  
NO<sub>x</sub>

K.-E. Min et al.

# Eddy covariance fluxes and vertical concentration gradient measurements of NO and NO<sub>2</sub> over a ponderosa pine ecosystem: observational evidence for within canopy removal of NO<sub>x</sub>

K.-E. Min<sup>1,\*</sup>, S. E. Pusede<sup>2</sup>, E. C. Browne<sup>2,\*\*</sup>, B. W. LaFranchi<sup>2,\*\*\*</sup>,  
P. J. Wooldridge<sup>2</sup>, and R. C. Cohen<sup>1,2</sup>

<sup>1</sup>University of California at Berkeley, Department of Earth and Planetary Science, Berkeley, CA, USA

<sup>2</sup>University of California at Berkeley, Department of Chemistry, Berkeley, CA, USA

\* now at: NOAA Earth System Research Laboratory and Cooperative Institute for Research in Environmental Sciences, University of Colorado, Boulder, USA

\*\* now at: Department of Civil & Environmental Engineering, Massachusetts Institute of Technology, Cambridge, MA, USA

\*\*\* now at: Lawrence Livermore National Lab, Center for Accelerator Mass Spectrometry (CAMS), Livermore, CA, USA

Title Page

Abstract

Introduction

Conclusions

References

Tables

Figures

⏪

⏩

◀

▶

Back

Close

Full Screen / Esc

Printer-friendly Version

Interactive Discussion



Received: 8 April 2013 – Accepted: 26 April 2013 – Published: 14 May 2013

Correspondence to: R. C. Cohen (rccohen@berkeley.edu)

Published by Copernicus Publications on behalf of the European Geosciences Union.

ACPD

13, 12437–12484, 2013

**Observational  
evidence for within  
canopy removal of  
NO<sub>x</sub>**

K.-E. Min et al.

Title Page

Abstract

Introduction

Conclusions

References

Tables

Figures



Back

Close

Full Screen / Esc

Printer-friendly Version

Interactive Discussion



## Abstract

Exchange of  $\text{NO}_x$  ( $\text{NO} + \text{NO}_2$ ) between the atmosphere and biosphere is important for air quality, climate change, and ecosystem nutrient dynamics. There are few direct ecosystem scale measurements of the direction and rate of atmosphere-biosphere exchange of  $\text{NO}_x$ . As a result, a complete description of the processes affecting  $\text{NO}_x$  following emission from soils and/or plants as they transit from within the plant/forest canopy to the free atmosphere remains poorly constrained and debated. Here, we describe measurements of  $\text{NO}$  and  $\text{NO}_2$  fluxes and vertical concentration gradients made during the Biosphere Effects on AeRosols and Photochemistry EXperiment 2009. In general, during daytime we observe upward fluxes of  $\text{NO}$  and  $\text{NO}_2$  with counter-gradient fluxes of  $\text{NO}$ . We find that  $\text{NO}_x$  fluxes from the forest canopy are smaller than calculated using observed flux-gradient relationships for conserved tracers and also smaller than measured soil  $\text{NO}$  emissions. We interpret these differences as evidence for the existence of a “canopy reduction factor”. We suggest that at this site it is primarily due to chemistry converting  $\text{NO}_x$  to higher nitrogen oxides within the forest canopy.

## 1 Introduction

The chemistry of nitrogen oxides is a major factor affecting the oxidative capacity of the atmosphere and the global burden of tropospheric ozone (Crutzen, 1973). Reactive nitrogen oxides are also a nutrient (Sparks, 2009; Takahashi et al., 2005a; Teklemariam and Sparks, 2004; Lockwood et al., 2008) and interactions between available nitrogen in ecosystems and atmospheric nitrogen are many and complex, with exchange processes altering the patterns of nitrogen availability in the biosphere (Townsend et al., 1996; Vitousek and Farrington, 1997; Vitousek et al., 1997; Holland and Lamarque, 1997; Holland et al., 1997; Ollinger et al., 2002a,b; Hietz et al., 2011). Nitrogen is the limiting nutrient for plant growth in most regions outside the tropics (Hungate et al.,

### Observational evidence for within canopy removal of $\text{NO}_x$

K.-E. Min et al.

Title Page

Abstract

Introduction

Conclusions

References

Tables

Figures

◀

▶

◀

▶

Back

Close

Full Screen / Esc

Printer-friendly Version

Interactive Discussion



## Observational evidence for within canopy removal of NO<sub>x</sub>

K.-E. Min et al.

Title Page

Abstract

Introduction

Conclusions

References

Tables

Figures

⏪

⏩

◀

▶

Back

Close

Full Screen / Esc

Printer-friendly Version

Interactive Discussion



2003; Galloway et al., 2004; Hietz et al., 2011), thus nitrogen deposited to the surface after atmospheric transport can act as fertilizer contributing to enhanced carbon uptake (Morikawa et al., 2004a,b; Takahashi et al., 2005a,b; Sparks, 2009; Norby et al., 2010). For example, Norby et al. (2010) found that the availability of nitrogen was a major limiting factor for the CO<sub>2</sub> fertilization effect in the FACE (Free-Air CO<sub>2</sub> Enrichment) experiment. However, too much nitrogen deposition may impair ecosystem health (Hessen et al., 1997; Herman et al., 2001) by causing dehydration, chlorosis, or membrane damage from peroxy acetal nitrate (PAN) (Ordin et al., 1971; Oka et al., 2004), or by inducing soil acidification and eutrophication (Makarov and Kiseleva, 1995; Pawlowski, 1997; Gbondo-Tugbawa and Driscoll, 2002; Zapletal et al., 2003; Chen et al., 2004).

A comprehensive understanding of NO<sub>x</sub> exchange between the atmosphere and biosphere does not yet exist. Experimental studies have primarily focused on NO emissions from soils to the atmosphere (e.g. Butterbach-Bahl et al., 2002; Gasche and Papen, 2002; Gut et al., 2002a,b; Rummel et al., 2002; van Dijk et al., 2002; Feig et al., 2008; Bargsten et al., 2010; Yu et al., 2010) or on the leaflevel transfer of NO and NO<sub>2</sub> using branch enclosures (Hereid and Monson, 2001; Chaparro-Suarez et al., 2011; Breuninger et al., 2013; and references therein). Studies at the canopyscale often assume simple flux-gradient similarity relationships – meaning molecular movement is always along the gradient from high to low concentration – to infer the rate of exchange from vertically resolved observations (Mayer et al., 2011 and reference therein). Direct measurements of the direction and rate of exchange, the flux, at the canopy scale are few (Wesely et al., 1982; Wildt et al., 1997; Horii, 2002; Horii et al., 2004; Farmer et al., 2006; Neiryneck et al., 2007; Li and Wang, 2009; Brummer et al., 2013).

The basic conceptual model for biosphere-atmosphere exchange of NO<sub>x</sub> is shown in Fig. 1. In this model, NO is mainly emitted by soil microbial activity, is converted to NO<sub>2</sub> by reaction with O<sub>3</sub>, and is then ultimately oxidized to nitric acid (HNO<sub>3</sub>), which returns back to the biosphere via wet and dry deposition. The timescale of NO to NO<sub>2</sub> conversion by O<sub>3</sub> and the photolysis of NO<sub>2</sub> back to NO is typically ~ 100 s in the daytime – comparable to that of the turbulent mixing time ( $\tau_{\text{turb}}$ ) within and out of a forest

**Observational  
evidence for within  
canopy removal of  
NO<sub>x</sub>**

K.-E. Min et al.

Title Page

Abstract

Introduction

Conclusions

References

Tables

Figures

⏪

⏩

◀

▶

Back

Close

Full Screen / Esc

Printer-friendly Version

Interactive Discussion

canopy. The timescale for NO<sub>x</sub> oxidation to HNO<sub>3</sub> by reaction of OH with NO<sub>2</sub> is 3–10 h, long enough that NO<sub>x</sub> changes by less than 1 % on the canopy residence time scale. The rapid interconversion between NO and NO<sub>2</sub> implies that the individual fluxes of NO or NO<sub>2</sub> will not be parallel to the fluxes of a conserved tracer, such as water, heat, or carbon dioxide (Vila-Guerau de Arellano et al., 1993), but the long lifetime of the sum implies the flux of NO<sub>x</sub> will parallel that of conserved tracers.

This model of NO<sub>x</sub> exchange is qualitatively supported by ecosystem scale observational studies. For example, NO is observed to decrease as air is transported up through a canopy from the forest floor (e.g. Rummel et al., 2002) and the low light levels within a shaded canopy reduce NO<sub>2</sub> photolysis and enhance the NO<sub>2</sub> to NO<sub>x</sub> ratio. For these reasons, downward NO fluxes and upward NO<sub>2</sub> fluxes have been observed as expected (e.g. Horii, 2002).

In contrast, calculations of ozone by large-scale chemical transport models parameterized with measured NO soil fluxes over-predict O<sub>3</sub> concentrations in comparison to aircraft and tower observations (e.g. Lerdau et al., 2000). To match observations, these models invoke a canopy reduction factor of 25–80 % (Jacob and Wofsy, 1990; Yienger and Levy, 1995; Wang and Leuning, 1998). This parameter functions non-mechanistically to remove soil NO<sub>x</sub> emission before it escapes the canopy, thus preventing its contribution to atmospheric ozone formation.

At the same time, laboratory observations at the leaf scale indicate bi-directional exchanges of NO<sub>x</sub> by plant biota, where the direction and rate of exchange is controlled by a so-called “compensation point” – a concentration above which vegetation takes up NO<sub>2</sub> and/or NO but below which emissions occur (Sparks et al., 2001; Raivonen et al., 2009; Chaparro-Suarez et al., 2011; Breuninger et al., 2013) but a mechanism for the emissions remains to be discovered (Breuninger et al., 2013). Direct observations of the NO<sub>2</sub> compensation point are analytically challenging (Raivonen et al., 2003) and evidence suggests that compensation behavior is not fixed but rather varies by plant species, plant lifecycle, and environmental conditions (Raivonen et al., 2009). That said, compensation points are measured in the range of ambient NO<sub>2</sub> abundances

## Observational evidence for within canopy removal of $\text{NO}_x$

K.-E. Min et al.

Title Page

Abstract

Introduction

Conclusions

References

Tables

Figures

⏪

⏩

◀

▶

Back

Close

Full Screen / Esc

Printer-friendly Version

Interactive Discussion



and have been reported from 0.05 to 3 ppb (Sparks et al., 2001; Raivonen et al., 2009; Chaparro-Suarez et al., 2011; Breuninger et al., 2013). Since the  $\text{NO}_2$  concentration in remote continental regions is typically less than 1 ppb these observations leave open the possibility that the majority of forests on Earth are a source of  $\text{NO}_x$ . This is in direct contradiction with the need for canopy reduction factors that remove nitrogen emitted from soils prior to its exit from plant canopies (Lerdau et al., 2000).

Recent field studies suggest the existence of rapid within-canopy chemistry affecting nitrogen oxides that is not included in the conceptual model of Fig. 1. Farmer et al. (2006) observed upward exchanges of total peroxy nitrates ( $\Sigma\text{RO}_2\text{NO}_2$ ) and  $\text{HNO}_3$  and interpreted this as the formation of these molecules within a forest canopy. In addition, Wolfe et al. (2009) described the importance of chemical processes in speciated acyl peroxy nitrate exchange also finding observational evidence for within-canopy chemistry affecting observed fluxes. Several other experimenters have reported the occurrence of within-canopy chemistry affecting fluxes of biogenic volatile organic compounds (BVOCs) (Holzinger et al., 2005; Karl et al., 2005; Bouvier-Brown et al., 2009a,b; Park et al., 2012) and ozone (Kurpius and Goldstein, 2003). Our own recent study of peroxy nitrate fluxes (Min et al., 2012), supports this idea, providing experimental evidence for upward fluxes of unidentified peroxy nitrates ( $F_{\text{XPN}}$ ) formed within the forest canopy. Taken together these studies emphasize the importance of rapid chemistry not only for determining the magnitude but also for the direction of nitrogen exchange at the biosphere-atmosphere interface.

The Biosphere Effects on AeRosols and Photochemistry EXperiment (BEARPEX) included a component designed to provide comprehensive measurements of concentrations, vertical gradients, and fluxes of a wide suite of nitrogen oxides –  $\text{NO}$ ,  $\text{NO}_2$ , total and speciated peroxy nitrates, total and speciated alkyl ( $\Sigma\text{RONO}_2$ ) and multifunctional nitrates,  $\text{HNO}_3$ , and nitrous acid (HONO) – and therefore presents a direct opportunity to test our ideas about canopy-scale  $\text{NO}_x$  exchange. Analyses of peroxy nitrate (Wolfe et al., 2009; Min et al., 2012) and HONO (Ren et al., 2011) fluxes have been reported elsewhere. Here we present observations of vertical concentration gradients

and fluxes of  $\text{NO}_2$  and  $\text{NO}$  measured with laser induced fluorescence and chemiluminescence, respectively. Fluxes are derived using the eddy covariance method. We describe relationships between gradients and fluxes, present and interpret evidence for a canopy reduction factor, and explore the significance of chemistry within the canopy to the import/export of  $\text{NO}_x$  from the canopy.

## 2 Research site and instrumentations

The data used in this work were obtained as a part of the BEARPEX 2009 experiment (15 June–31 July 2009). The experiment was conducted over a managed Ponderosa pine plantation on the western slope of the Sierra Nevada Mountain range, 75 km downwind of Sacramento, California and near the University of California Berkeley Blodgett Forest Research Station (UC-BFRS,  $38^\circ 53' 42.9''$  N,  $120^\circ 37' 57.9''$  W, 1315 m). Many of the results from BEARPEX can be found in a special issue of Atmospheric Chemistry and Physics, [http://www.atmos-chem-phys-discuss.net/special\\_issue89.html](http://www.atmos-chem-phys-discuss.net/special_issue89.html). A brief description of the field site and of the instrumentation relevant to this paper follows.

Analysis of the local meteorology by Choi et al. (2011) and Dillon et al. (2002) indicate that in the summer (May–September), winds at the BEARPEX site are characterized by daytime southwesterlies ( $210$ – $240^\circ$ ) and nighttime northeasterlies ( $30^\circ$ ) with little variability. The major source of anthropogenic emissions in the region is the city of Sacramento and its suburbs. There is a line source of Oak trees that are strong isoprene emitters aligned perpendicular to the flow between the urban center and the site. This source distribution in combination with the regular winds results in low concentrations of trace gases with anthropogenic or isoprene sources early in the morning and higher concentrations in air transported from the west later in day. The two sources arrive at distinct times; with air influenced primarily by isoprene arriving at approximately noon and the urban plume combined with the isoprene source arriving about 3–4 h later.

Observational  
evidence for within  
canopy removal of  
 $\text{NO}_x$

K.-E. Min et al.

Title Page

Abstract

Introduction

Conclusions

References

Tables

Figures

⏪

⏩

◀

▶

Back

Close

Full Screen / Esc

Printer-friendly Version

Interactive Discussion



## Observational evidence for within canopy removal of NO<sub>x</sub>

K.-E. Min et al.

Title Page

Abstract

Introduction

Conclusions

References

Tables

Figures

⏪

⏩

◀

▶

Back

Close

Full Screen / Esc

Printer-friendly Version

Interactive Discussion

There were two sampling towers at the site; a 15 m walk-up tower on the south side of the site (hereafter south tower), and 18 m scaffolding tower located 10 m north of the south tower (hereafter north tower). On south tower, temperature, relative humidity, wind speed, net radiation, photosynthetically active radiation (PAR), water vapor, carbon dioxide (CO<sub>2</sub>), and O<sub>3</sub> were monitored at 5 heights (1.2, 3.0, 4.9, 8.75, and 12.5 m above the forest floor). At 12.5 m, fluxes of water vapor, CO<sub>2</sub>, and O<sub>3</sub> were measured. Vertical gradients of temperature, relative humidity, and wind speed were also measured on the north tower at 5 heights (1.2, 5.4, 9.2, 13.3, and 17.5 m above the forest floor). Measurements from the north tower or on an adjacent height adjustable lift included NO, NO<sub>2</sub>, HONO, total peroxy nitrates (ΣPNs, RO<sub>2</sub>NO<sub>2</sub>), total alkyl and multifunctional nitrates (ΣAN, RONO<sub>2</sub>), HNO<sub>3</sub>, hydroxyl radical (OH), hydroxy peroxy radical (HO<sub>2</sub>), OH reactivity, O<sub>3</sub>, several individual PNs, several individual ANs, numerous volatile organic compounds (VOCs) including many biogenic VOCs (BVOCs), formaldehyde (HCHO), glyoxal, methylglyoxal, organic peroxides, and aerosol chemical and physical properties. Needle temperature, soil moisture, soil temperature, and soil heat flux were also monitored. In addition, soil NO emissions were measured using dynamic chamber on 2, 12 and 30 July. All measurements were made at the 17.5 m level and many were additionally recorded at one or more of the following heights: 0.5, 1.2, 5.4, 9.2, and 13.3 m. For simplicity, we refer to these measurement heights as 0.5, 1, 5, 9, 13 and 18 m.

The upper canopy at this site was mainly *Pinus ponderosa* L., with a few scattered Douglas fir, white fir, and incense cedar. The understory was primarily mountain whitethorn (*Ceanothus cordulatus*) and manzanita (*Arcostaphylos species*) shrubs (see Misson et al., 2005, for a more detailed site description and history). The mean tree height was 8.8 m and the leaf area index (LAI) was 3.7 m<sup>2</sup> m<sup>-2</sup> based on a tree survey conducted on 17 July 2009.

NO was measured using a custom built twochannel chemiluminescence NO detection system (2ch-CL) and NO<sub>2</sub> with two separate thermal dissociation laser-induced fluorescence (TD-LIF) systems. The sampling inlets for NO and NO<sub>2</sub> were collocated



**Observational  
evidence for within  
canopy removal of  
NO<sub>x</sub>**

K.-E. Min et al.

Title Page

Abstract

Introduction

Conclusions

References

Tables

Figures

⏪

⏩

◀

▶

Back

Close

Full Screen / Esc

Printer-friendly Version

Interactive Discussion

at 0.5, 5, 9 and 18 m on the north tower and represent the forest floor, mid canopy, top canopy, and above canopy, respectively. At 18 m, fluxes of NO and NO<sub>2</sub> were monitored along with 3-D wind and temperature from a sonic anemometer (Campbell Scientific CSAT3 3-D Sonic Anemometer). The measurements were combined to infer fluxes using eddy covariance method (EC) (see Sect. 3). The sonic anemometer was pointing into the mean daytime wind stream with 0.02 m vertical displacement and 0.2 m horizontal displacement from the NO and NO<sub>2</sub> inlets.

The 2ch-CL system for the NO flux and vertical gradient measurements was based on the standard O<sub>3</sub> chemiluminescence method. A detailed description of the operating principle can be found elsewhere (Drummond et al., 1985 and references therein). Briefly, ambient NO is combined with an excess of O<sub>3</sub> (generated by electric discharge in O<sub>2</sub>). The reaction of NO and O<sub>3</sub> produces excited state NO<sub>2</sub> molecules, which then fluoresce. One of the gold-plated detection cells was used for the flux measurement and the other one cell for the vertical concentration gradient measurement. The signals from photocathodes (flux channel: EMI 9658B, gradient channel: Hamamatsu H7421-50) were acquired at 5 Hz. The cell pressures were maintained at 8–8.7 Torr with pressure restricted at the inlet and a fluorinated oil-sealed rotary vane pump. During the sampling mode, 100 % of the ozone flow was added directly into the detection cell to monitor the ambient NO concentration (for 24 s). The background signal was monitored by adding 50 % of the O<sub>3</sub> to the sampling air prior to the detection cell to titrate ~ 90 % NO (for 6 s). Incomplete titration of NO was employed to limit interferences from fluorescence of vibrationally excited OH molecules produced in the reaction of ozone with alkenes (Drummond et al., 1985). The other 50 % of the ozone was added directly to the cell to minimize flow changes within the reaction cell between the sampling and the background mode. Our own laboratory experiments confirm that a wide variety of terpenes react with ozone to efficiently produce vibrationally excited OH and we configured the instrument to minimize detection of this signal.

Two TD-LIF systems were used for simultaneous flux and vertical gradient measurements of NO<sub>2</sub> and the higher nitrogen oxide species ΣPNs, ΣANs and HNO<sub>3</sub>. Details

**Observational  
evidence for within  
canopy removal of  
NO<sub>x</sub>**

K.-E. Min et al.

Title Page

Abstract

Introduction

Conclusions

References

Tables

Figures

⏪

⏩

◀

▶

Back

Close

Full Screen / Esc

Printer-friendly Version

Interactive Discussion

of LIF detection of NO<sub>2</sub> (Thornton et al., 2000), thermal dissociation of higher nitrogen oxides (Day et al., 2002) and application to EC flux measurement (Farmer et al., 2006) are described elsewhere. Briefly, thermal dissociation of each class of higher oxide generates NO<sub>2</sub> and a companion radical at the characteristic temperatures ~ 180 °C for ΣPNs, ~ 350 °C for ΣANs, and ~ 600 °C for HNO<sub>3</sub>, (Day et al., 2002). The thermal dissociation is followed by detection of NO<sub>2</sub> by LIF. In both TD-LIF systems, excitation at 585 nm was provided by frequency doubled Nd : YAG (Spectra Physics, average power of 2 W at 532 nm, 30 ns pulse length) pumping a custom-built tunable dye laser operating at 8 kHz. The wavelength of the dye laser beam was tuned to a specific, narrow rovibronic feature of NO<sub>2</sub> by rotating an etalon within the dye cavity. We alternated the laser frequency between a strong NO<sub>2</sub> resonance (8 s) and the weak continuum adsorption (4 s) to maintain a frequency lock on the spectral feature of interest. By adapting a supersonic expansion technique, we acquired ~ 10-fold higher sensitivity to NO<sub>2</sub> (Cleary et al., 2002). The fluorescence signal long of 700 nm was collected and imaged onto a red sensitive photocathode (Hamamatsu H7421-50) and gated photon counting techniques (Stanford Research Systems, SRS 400) were employed to discriminate against prompt background signals. Laboratory measurements and comparison in the field showed the two TD-LIF instruments to have calibrations that were identical to within 4 % (slope:  $1.0 \pm 0.10$ ,  $R^2$ : 0.92). Allowing the intercept to vary from zero did not change the slope and  $R^2$ .

The cell pressures in the flux system were reduced to 0.17–0.19 Torr to achieve the high expansion ratios for the supersonic jet cooling by using Lysholm twin screw blowers (Whipple model 2300 superchargers) backed by an oil-sealed rotary vane pump. The jet nozzles and this pump system combined to maintain a 580–700 sccm flow through each of the four cells (total flow of 2300 sccm). To reduce high frequency damping of turbulent eddies and interference from secondary chemistry in the heated section of the inlet and sampling lines (30 m), we added a diaphragm bypass pump and maintained the total flow of a 13 000 sccm. For the gradient system, critical orifices as

pressures restrictors (AirLogic, F-2815-251-B85, 0.025" orifice diameter) were placed at the end of the inlet manifold to reduce the pressure along the sampling line.

Calibrations in the field were repeated once (gradient measurement of NO and NO<sub>2</sub> and flux measurement of NO) or twice (flux measurement of NO<sub>2</sub>) per hour for both the NO and NO<sub>2</sub> instruments. NO<sub>2</sub> standard gas (4.9 ± 0.2 ppm NO<sub>x</sub> in N<sub>2</sub>, PRAX-AIR) was diluted to 3–20 ppb in zero air and added to system at the inlet tip. For NO, 2.25–6.7 ppb of NO (5.4 ppm ± 5% NO in N<sub>2</sub>, PRAXAIR) was diluted with zero air and added at the inlet. Both cylinders were referenced to a library of calibration standards maintained in our laboratory. The mixing ratios were corrected (< 2%) for quenching by water using the north tower RH measurement. To evaluate the background counts due to cell scatter and photocathode dark noise, we flowed excess zero air into the inlet once/twice per hour. The diagnostics for the NO and NO<sub>2</sub> flux instruments (calibration and zeroing) were completed within the first 3 min of every 30 min (Fig. 2a). Flux data for both species were collected at 18 m during the first 30 min, from the 3rd minute to the 30th minute, and for the last 30 min, from the 33rd minute to the 60th minute each hour (Fig. 2a). NO and NO<sub>2</sub> at the lower levels were measured by switching between the 9, 5, and 0.5 m heights and sampling at each height for 2 min (Fig. 2b). Calibrations and zeros were completed in last 4 min from 56th to 60th minutes of every hour for both gradient systems (Fig. 2b).

Data affected by exhaust plumes from a nearby propane electrical generator (mostly at night) and the infrequent wafts of car exhaust were removed prior to analysis. These spikes were defined as variations in the NO or NO<sub>2</sub> concentration in excess of 3 times the standard deviation of the 10 min running mean. A few remaining spikes were identified through correlations with CO and removed by hand. Over the campaign, the NO<sub>2</sub> detection limit (defined as  $S/N = 2$ ) was ~45 ppt (1 s) for the flux system and was ~10 ppt (1 min) for gradient system. The NO detection limit for flux cell was ~58 ppt (1 s) and for gradient cell was ~29 ppt (1 min) in midday (12:00–14:00 LT). Local Time (Pacific Standard Time) is used throughout this paper.

**Observational  
evidence for within  
canopy removal of  
NO<sub>x</sub>**

K.-E. Min et al.

Title Page

Abstract

Introduction

Conclusions

References

Tables

Figures

⏪

⏩

◀

▶

Back

Close

Full Screen / Esc

Printer-friendly Version

Interactive Discussion



### 3 Eddy-covariance calculation

The flux ( $F_c$ ) of an atmospheric constituent ( $c$ ), i.e. the turbulent mass transport of  $c$  through a vertical reference layer, can be evaluated from the covariance between the concentration of  $c$  and the vertical wind ( $w$ ) in a method known as eddy-covariance (EC) and is represented mathematically by Eq. (1) (e.g. Foken, 2006; Lee et al., 2004; McMillen, 1988):

$$F_c = \int_{t_0}^t w' c' dt = \frac{1}{n} \sum_{i=1}^n (w_i - \bar{w})(c_i - \bar{c}) = \overline{w' c'} \quad (1)$$

In Eq. (1), the primes represent the deviation from the mean, the subscripts  $i$  refer to individual hightime resolution measurements ( $\text{NO}$  or  $\text{NO}_2$ ), and the bar indicates the mean over the averaging interval. In this work, the flux of  $\text{NO}_x$ ,  $F_{\text{NO}_x}$ , is defined as the sum of the separately calculated  $F_{\text{NO}}$  and  $F_{\text{NO}_2}$ .

We used 5 Hz data for the flux calculations and averaged for  $\sim 30$  min – a time scale that spanned the range of the major flux-carrying eddies at this site (e.g. Wolfe et al., 2009; Farmer et al., 2006). Prior to calculating fluxes, we rotated the wind measurements to ensure that the vertical winds were normal to the shear plane (Baldocchi et al., 1988; McMillen, 1988). We also de-spiked and de-trended the concentration data, where spikes were defined as data greater than 3 times the standard deviation of the 10 min running mean, and where the 10 min running mean was also used for de-trending.

To synchronize the timing of wind and concentration measurements, the lag was determined from the maximum in covariance of the deviation from the mean of vertical wind speed and concentration. Figure 3a–c show the lag correlation between wind and temperature,  $\text{NO}$ , and  $\text{NO}_2$ , respectively. The data plotted in Fig. 3 are the averaged midday (12:00–14:00) lag over the whole field campaign. As expected, 0 lag was observed between vertical wind speed and temperature since both quantities are synchronously measured by same instrument, the sonic anemometer. Lag times for  $\text{NO}$

and  $\text{NO}_2$  were measured to be 1.4 s and 2.6 s, times that were consistent with transport times in the tubing ( $< 0.8$  s) plus the time difference between sonic anemometer computer and computers for 2ch-CL and TD-LIF.

To assure that each 30 min flux was representative of the average surface exchange over the sampling period, we tested the calculated fluxes for stationarity (Farmer et al., 2006; Foken, 2006; Wolfe et al., 2009). To do this, five equally divided subsets of each 30 min flux period,  $F_{\text{sub}}$ , were averaged and compared with that of the full period,  $F_{30 \text{ min}}$ . If  $F_{\text{sub}}$  differed from  $F_{30 \text{ min}}$  by more than 30 % then that measurement period was defined as non-stationary and that half hour excluded from further analysis (Foken and Wichura, 1996). Also, the calculated flux data with a tilt angle greater than  $5^\circ$  from the wind rotation (Lee et al., 2004) and with a friction velocity smaller than  $0.1 \text{ ms}^{-1}$  or larger than  $1.5 \text{ ms}^{-1}$  (Foken, 2006) were excluded for further analysis. Approximately 2/3 of the daytime and half of the nighttime data remained after application of these filters. We estimate the total uncertainty in  $F_{\text{NO}_x}$  by combining the systematic and random error terms in  $F_{\text{NO}}$  and  $F_{\text{NO}_2}$  flux estimations followed by Moore et al. (1986) and Massman (1991). Each of the individual elements is summarized in Table 1 and detailed procedures are described in Farmer et al. (2006) and Wolfe et al. (2009).

The total systematic uncertainties for  $F_{\text{NO}}$  and  $F_{\text{NO}_2}$  ( $< 8\%$  and  $< 6\%$ ) are calculated from the root mean square of errors from instrument calibration (7% and 5% for NO and  $\text{NO}_2$ , see Day et al., 2002), sensor separation and inlet dampening ( $< 2\%$  for both  $F_{\text{NO}}$  and  $F_{\text{NO}_2}$ ), instrument time response ( $< 0.2\%$  and  $< 0.7\%$  for daytime  $F_{\text{NO}}$  and  $F_{\text{NO}_2}$ ) and data acquisition sequencing (i.e. laser line-locking cycling for TD-LIF system:  $< 3\%$  or frequent background checking for 2ch-CL system:  $< 2\%$ , estimated from the sensible heat flux calculation using temperature data coincident with the NO or  $\text{NO}_2$  data).

Two different methods were used to estimate the precision (random errors) of the flux measurements: (1) estimates based on the finite precision of photon counting and (2) the variance of the flux calculation with lag determination. The precision estimates based on photon counting statistics follow Farmer et al. (2006) and are  $0.08 \text{ ppt ms}^{-1}$

**Observational  
evidence for within  
canopy removal of  
 $\text{NO}_x$** 

K.-E. Min et al.

Title Page

Abstract

Introduction

Conclusions

References

Tables

Figures

◀

▶

◀

▶

Back

Close

Full Screen / Esc

Printer-friendly Version

Interactive Discussion



## Observational evidence for within canopy removal of $\text{NO}_x$

K.-E. Min et al.

Title Page

Abstract

Introduction

Conclusions

References

Tables

Figures

⏪

⏩

◀

▶

Back

Close

Full Screen / Esc

Printer-friendly Version

Interactive Discussion

refer to negative and solid lines to positive cospectral density. Few studies report sign changes in a scalar cospectrum other than that of momentum flux (Wolfe et al., 2009; Park et al., 2013). Details of the cospectral analysis along with sign changes and the discussion of their underlying physical mechanisms will be presented elsewhere (Min et al., 2013). Briefly, we find that chemical reactions forming higher oxides of nitrogen from  $\text{NO}_x$  are one possible cause of frequent sign change only in scalar co-spectrum. The normalized cospectrum, shown in Fig. 4b, indicates the fraction of the total flux at each frequency. It is calculated as the cospectra multiplied by the frequency and divided by the covariance of temperature, or  $\text{NO}_x$ , with the vertical wind, which is the integrated value under the curve. Generally, the shape of the normalized cospectrum of  $w'\text{NO}_x'$  is similar to that of  $w'T'$  with a maximum in the range 0.005–0.1 Hz (200–10 s), values consistent with previous observations at this site (Farmer et al., 2006; Wolfe et al., 2009; Park et al., 2012). A steeper falloff at high-frequencies ( $> 0.01$  Hz) for  $w'\text{NO}_x'$  (especially in the afternoon, not shown) than for  $w'T'$  was reported in previous studies of PAN at this site (Wolfe et al., 2009) and in a Loblolly pine forest (Turnipseed et al., 2006) as well as for a variety of BVOCs at this site (Park et al., 2012). The deep feature seen at frequencies of 0.001–0.005 Hz is associated with cospectrum sign changes (shown as  $\blacktriangle$  for negative sign in Fig. 4).

Figure 4c shows the normalized cumulative distributions of the cospectra and ogives of  $w'T'$  and  $w'\text{NO}_x'$ . The ogive for  $w'T'$  approaches a horizontal asymptote at both ends of the spectrum, providing additional confirmation that the sampling interval and time resolution was both long enough and fast enough to capture all the important flux-carrying eddies. The ogive pattern of  $w'\text{NO}_x'$  is generally comparable to that of  $w'T'$ , except for frequencies in the ranges 0.001–0.005 Hz and 0.1–1 Hz, where cospectrum signs are negatives. Here, we use the the frequency weighted normalized cospectrum of  $w'\text{NO}_x'$  for the ogive calculation noting that the frequencies of  $w'\text{NO}_x'$  that are have a negative cospectrum vary with time of day, suggesting they are not internally generated, but are rather the result of time-of-day dependent atmospheric processes. Detailed discussion of these features will be presented elsewhere (Min et al., 2013).

## 4 Gradients and fluxes

The diurnal variations in the concentrations of  $O_3$ ,  $NO_x$ ,  $NO$ , and  $NO_2$  are shown in Fig. 5 and are similar to previous observations at this site (Day et al., 2003; Farmer et al., 2006). The patterns are affected by transport from Sacramento, emissions from soils, deposition, and chemistry.  $O_3$ ,  $NO_x$ , and  $NO_2$  increase as air is transported from the west carrying the remnants of emissions from the Sacramento metropolitan area and reach a maximum after sunset between 18:00 to 21:00. Generally,  $NO$  can be thought of as controlled by the amount of  $NO_x$  and local photochemistry. In the morning, we observe enhancements in  $NO$  and  $NO_2$  and a decrease in  $O_3$ . Vertical gradients are also present. We observe the highest  $NO$  concentrations above the canopy, decreasing  $NO$  within the forest canopy and increasing  $NO$  concentrations again near the forest floor – except in the late afternoon when turbulent mixing is strongest and dry soils result in  $NO$  emissions that are at their daily minimum.

Typical  $NO$  mixing ratios above the canopy during BEARPEX 2009 ranged from 10 to 100 ppt with a daytime (09:00–18:00) mean ( $\pm 1\sigma$ ) of  $45 \pm 19$  ppt. This concentration is  $\sim 20\%$  lower than observed at this site during same time of year in 2001 (Day et al., 2003). The highest  $NO$  concentration near the forest floor was 270 ppt following rainfall on the evening of day 192 (11 July). The mixing ratio of  $NO_2$  above the canopy varied from 80 to 550 ppt with a daytime mean concentration of  $188 \pm 86$  ppt. This is a 65% decrease from the 533 ppt mean observed in 2001 (Day et al., 2003) and is in agreement with previously reported  $NO_x$  decreases in upwind Sacramento of approximately 13%/yr, which accumulate to an approximately 67% decrease between 2001 and 2009 (Russell et al., 2010; LaFranchi et al., 2011).

Figure 6 shows the vertical gradients of  $NO$ ,  $NO_2$ , and  $NO_x$  throughout the course of the day: early morning (06:00–09:00, blue), late morning (09:00–12:00, cyan), midday (12:00–14:00, red), afternoon (14:00–18:00, magenta), evening (18:00–24:00, green) and night (24:00–06:00, black). For the purpose of discussion we define an enhancement factor ( $\Delta X$ ) to be the concentration difference between each height and that

### Observational evidence for within canopy removal of $NO_x$

K.-E. Min et al.

Title Page

Abstract

Introduction

Conclusions

References

Tables

Figures

⏪

⏩

◀

▶

Back

Close

Full Screen / Esc

Printer-friendly Version

Interactive Discussion



## Observational evidence for within canopy removal of $\text{NO}_x$

K.-E. Min et al.

Title Page

Abstract

Introduction

Conclusions

References

Tables

Figures

⏪

⏩

◀

▶

Back

Close

Full Screen / Esc

Printer-friendly Version

Interactive Discussion

measured above the canopy ( $\Delta X = X_i - X_{18m}$ ). Positive values of  $\Delta X$  indicate concentration enhancements and negative values indicate depleted concentrations relative to above the canopy. As shown in Fig. 6, NO was depleted within the canopy (a) and  $\text{NO}_2$  was enhanced at all times of day (b). In general, we observed the least NO depletion near the soil (except for night time) and larger  $\text{NO}_2$  enhancements at mid- and top-canopy heights. This pattern is qualitatively explained by emissions of NO at the soil followed by the conversion of NO to  $\text{NO}_2$  until the steady-state ratio is established by the reaction of NO with  $\text{O}_3$  and photolysis of  $\text{NO}_2$ .

If soil NO emissions and the chemical cycling of NO/ $\text{NO}_2$  were the only two process controlling  $\text{NO}_x$ , then we would expect the gradient in the sum of NO and  $\text{NO}_2$  to be a straight line connecting the enhanced concentration at forest floor with the above canopy (boundary layer value) so long as sufficient turbulent mixing exists (Vila-Guerau de Arellano et al., 1993; Gao et al., 1991; Jacob and Wofsy, 1990). This, however, is not what we observe (Fig. 6c). Rather we observe a  $\text{NO}_x$  enhancement during daytime and depletion during nighttime within the canopy. In addition, the enhancement at the forest-floor, mid-canopy, and top-canopy heights changes within different time windows, indicating the existence of multiple processes other than soil NO emission and simple inter conversion of NO and  $\text{NO}_2$ . For example, the within-canopy gradients at 06:00–09:00 (blue) and 14:00–18:00 (magenta) are opposite each other; the 06:00–09:00  $\text{NO}_x$  gradient indicates the existence of a  $\text{NO}_x$  sink process as the height increases from mid to top-canopy, while the 14:00–18:00 gradient indicates a  $\text{NO}_x$  source. While there have been a number of indirect lines of evidence for the idea of that processes other than soil NO emission and NO/ $\text{NO}_2$  photochemical partitioning affect  $\text{NO}_x$  fluxes (Jacob and Wofsy, 1990; Yienger and Levy, 1995; Wang and Leuning, 1998; Lerday et al., 2000; Wolfe et al., 2011; Min et al., 2012a), to our knowledge these observations provide the first direct observational evidence.

In Fig. 7a–c, we show the eddy-covariance fluxes of NO,  $\text{NO}_2$  and  $\text{NO}_x$ . We observed upward fluxes from 09:00 to 15:00. Fluxes of NO and  $\text{NO}_x$  were slightly downward from 06:00–09:00. The midday (12:00–14:00) median fluxes of NO,  $\text{NO}_2$  and  $\text{NO}_x$  are

**Observational  
evidence for within  
canopy removal of  
NO<sub>x</sub>**

K.-E. Min et al.

Title Page

Abstract

Introduction

Conclusions

References

Tables

Figures

⏪

⏩

◀

▶

Back

Close

Full Screen / Esc

Printer-friendly Version

Interactive Discussion

0.32 ± 0.27 , 0.67 ± 0.21 and 1.0 ± 0.43 pptms<sup>-1</sup>. A comparison of the direction of the observed flux of NO<sub>2</sub> and NO<sub>x</sub> to the gradients in Fig. 6b, c gives a picture of molecular movement consistent with standard ideas of turbulent transport moving material from a region of high to low concentration. For NO, however, the direction of the flux is counter to that of the concentration gradient.

The observed midday fluxes of NO<sub>x</sub> of 1.0 ± 0.43 pptms<sup>-1</sup> are smaller than the lower end of soil NO emission measured at this site (3 ± 3 pptms<sup>-1</sup> in the morning) and smaller than other soil NO<sub>x</sub> studies in the region. Our own measurements were in a nearby clearing and may have been in soil that was drier, and hence has a lower soil NO<sub>x</sub> emission, than is representative of the fetch at the site. At the Schubert Watershed at the Sierra Nevada Foothill Research and Extension Center in an oak forest, soil NO<sub>x</sub> emissions of 5.8–15 pptms<sup>-1</sup> were observed during the summer (Herman et al., 2003) and typical soil NO fluxes reported for other locations in California are 2–20 pptms<sup>-1</sup> (Anderson and Poth, 1989; Davidson et al., 1993). Comparison of these soil NO<sub>x</sub> emissions to our ecosystem scale flux measurements suggests the existence of NO<sub>x</sub> removal process within the canopy – a NO<sub>x</sub> canopy reduction factor.

To evaluate the contribution of soil NO emission to the NO<sub>2</sub> flux by the reaction with O<sub>3</sub>, we divide our system into a soil NO emission layer and a chemical conversion layer, where the latter layer includes the within and above canopy measurement heights. The noontime (12:00–14:00) ratio of NO and NO<sub>2</sub> in the conversion layer (estimated as the averaged value over all measured heights) is 1 : 4.7 indicating 0.82 NO<sub>2</sub> molecules are produced for every NO molecule emitted from soil emission layer. Using the lowest measured soil NO emission rate and the observed O<sub>3</sub> at this site, we calculate conversion of NO to NO<sub>2</sub> induces a 2.38 pptms<sup>-1</sup> NO<sub>2</sub> flux, a number which is 3.5 times larger than the observed NO<sub>2</sub> flux (0.67 ± 0.21 pptms<sup>-1</sup>), another piece of evidence supporting the existence of a canopy reduction process for NO<sub>2</sub>.

## 5 Analysis

For a conserved tracer, the direction and magnitude of the flux is controlled by the local concentration gradient and the rate of vertical mixing – the tracer moving from high to low abundance and the rate of movement determined by the strength of both the gradient and the turbulent mixing. This concept is known as flux-gradient similarity or Bowen ratio theory, and is often used for estimating the exchange rate of non-reactive (conserved) species from their concentration gradient (e.g. Mayer et al., 2011 and references therein). Similarity theory holds for conserved tracers when observations of fluxes are made above the roughness sublayer (Raupach and Legg, 1984) and this criterion was met at BEARPEX 2009 (18 m flux measurement height with 8.8 m mean tree height), as evidenced by a comparison of the flux data of the sensible heat and 3 biogenic VOC species (methanol, 2-methyl-3-butene-2-ol + isoprene and monoterpene) with longer chemical lifetimes than the turbulent transport time (Park et al., 2012).

The fluxes of reactive species cannot be completely described through simple application of similarity theory. This is because reactive species will, to some extent, undergo chemical transformations faster than they will be transported by turbulent diffusion (Vila-Guerau de Arellano et al., 1993; Gao et al., 1991; Jacob and Wofsy, 1990). However, similarity theory is still a powerful tool, as quantifying the flux due to turbulence transport, allows estimation of the effects of other within-canopy chemical processes.

A visual representation of the idea proposed in this study is shown in Fig. 8. The red line shows the gradient expected if flux-gradient similarity holds and the blue line shows the gradient if the concentration is chemically, or otherwise, perturbed. This is known as Localized Near-Field (LNF) theory (Vandenhurk and Mcnaughton, 1995; Raupach, 1989). In the analysis below, we will assess the within-canopy behavior of NO, NO<sub>2</sub>, and NO<sub>x</sub> through pictorial relationships analogous to Fig. 8.

In Fig. 8, the green dashed line divides two layers: a within canopy layer and an above-canopy layer.  $C_{\text{ABOVE}}$  is the measured concentration in the above canopy

**Observational  
evidence for within  
canopy removal of  
NO<sub>x</sub>**

K.-E. Min et al.

Title Page

Abstract

Introduction

Conclusions

References

Tables

Figures



Back

Close

Full Screen / Esc

Printer-friendly Version

Interactive Discussion



layer and  $C_{\text{WITHIN}}$  is the measured concentration within the canopy. Using similarity theory and the measured fluxes we calculate  $C_{\text{CONSERVED}}$ , the concentration that would be observed for a conserved tracer. The difference between  $C_{\text{WITHIN}}$  and  $C_{\text{CONSERVED}}$ , defines  $C_{\text{DELTA}}$ , which represents the contribution to the concentration by non-conservative processes that act to perturb the flux gradient relationship. To quantify  $C_{\text{CONSERVED}}$  we use flux-gradient similarity, Eq. (2), (Meyer, 1986) and the mixing rate,  $K$ , the so called the eddy diffusivity constant, which is inferred from the observed sensible heat flux and temperature gradient.

$$\frac{\partial(C_{\text{CONSERVED}} - C_{\text{ABOVE}})}{\partial z} = \frac{\text{Flux}}{K} \quad (2)$$

In an illustrative test of our approach we present our results for the conserved tracer water. In Fig. 9, the blue circles represent the measured gradient of  $\text{H}_2\text{O}$  and the red circles show the gradient inferred from the  $\text{H}_2\text{O}$  flux ( $C_{\text{CONSERVED}}$ ) in the within-canopy layer at midday (12:00 to 14:00 h). As expected, the difference between  $C_{\text{WITHIN}}$  and  $C_{\text{CONSERVED}}$  in the within-canopy layer,  $C_{\text{DELTA}}$ , shown as a black arrow, is small (1 % relative to  $C_{\text{ABOVE}}$  and within the concentration measurement uncertainty of 3 %). This implies there is no measureable additional source/sink process(es) for  $\text{H}_2\text{O}$  aside from turbulent transport. Similar results were obtained for  $\text{CO}_2$  and several slowly reacting BVOC.

Applying the same analysis to NO and  $\text{NO}_2$  (Fig. 10), we find  $C_{\text{DELTA}}$  is large compared to the measurement variability.  $C_{\text{DELTA}}$  for NO is  $-12.4 \pm 3.3$  ppt (23 % relative to  $C_{\text{ABOVE}}$ ) and for  $\text{NO}_2$  is  $64.7 \pm 4.7$  ppt (44 % relative to  $C_{\text{ABOVE}}$ ). We reach an identical conclusion, with slight numerical differences, if we reference the calculation to the canopy top height instead of the average through the canopy; 27 % and 39 % of difference for NO and  $\text{NO}_2$  to the  $C_{\text{ABOVE}}$ , respectively.

Based on the observed gradient of NO, standard flux-gradient similarity predicts the downward flux of NO; however, we observed an upward flux of NO (Fig. 7). This counter-gradient flux can only be explained by the formation of NO during the transport process from within the canopy layer to the above canopy layer. Figure 10a indicates

**Observational evidence for within canopy removal of  $\text{NO}_x$**

K.-E. Min et al.

Title Page

Abstract

Introduction

Conclusions

References

Tables

Figures

⏪

⏩

◀

▶

Back

Close

Full Screen / Esc

Printer-friendly Version

Interactive Discussion



## Observational evidence for within canopy removal of NO<sub>x</sub>

K.-E. Min et al.

Title Page

Abstract

Introduction

Conclusions

References

Tables

Figures

⏪

⏩

◀

▶

Back

Close

Full Screen / Esc

Printer-friendly Version

Interactive Discussion



that to explain the observed NO flux, we need to account for 12 ppt ( $C_{\text{DELTA}}$ ) more NO molecules than were observed in the canopy layer. This is reasonable as photolysis rates above the canopy should be faster than in the shade of the canopy. If the required NO were completely due to NO<sub>2</sub> photolysis it would correspond to ~ 12 ppt removal (20 % of the  $C_{\text{DELTA}}$ ) of NO<sub>2</sub>. The remainder (80 % of  $C_{\text{DELTA}}$  in NO<sub>2</sub>, 52.3 ppt) must be accounted for via other mechanisms.

To evaluate the contribution of photolysis of NO<sub>2</sub> to the counter-gradient flux of NO, we calculate the chemical conversion rate integrated over the 100 s ( $\tau_{\text{turb}}$ ) as Eq. (3).

$$P_{\text{NO,net}} = L_{\text{NO}_2,\text{net}} = j_{\text{NO}_2} \text{NO}_2 - (k_{\text{NO}+\text{O}_3}[\text{O}_3] + k_{\text{NO}+\text{HO}_2}[\text{HO}_2] + k_{\text{NO}+\text{RO}_2}[\text{RO}_2])[\text{NO}] \quad (3)$$

The photolysis rate,  $j_{\text{NO}_2}$ , is calculated with the Tropospheric Ultraviolet and Visible (TUV) radiation model scaled to the measured PAR. We treat RO<sub>2</sub> as equal to HO<sub>2</sub>. Using the measured concentrations of NO, NO<sub>2</sub>, O<sub>3</sub>, HO<sub>2</sub>, and temperature, we estimate a net loss of 22.8 ppt of NO<sub>2</sub>, which is in excess of that needed to explain the NO counter-gradient flux of 12.4 ( $\pm 3.3$ ) ppt.

The large value of  $C_{\text{DELTA}}$  for NO<sub>x</sub> ( $54.3 \pm 5.9$  ppt, 29 % relative to  $C_{\text{ABOVE}}$ ) indicates the necessity of one or more within-canopy loss processes. To explore the mechanism(s) controlling the  $C_{\text{DELTA}}$  for NO<sub>x</sub>, we examine several chemical processes related to PNs, ANs, HNO<sub>3</sub>, and HONO using our two-layer model (concept shown in Fig. 8). The magnitudes of each of the near-field processes for NO<sub>x</sub> were inferred using Eq. (4) to estimate the contribution of certain processes on the ~ 100 s timescale of turbulent mixing ( $\tau_{\text{turb}}$ ).

$$L_x \text{ or } P_x = \frac{\partial}{\partial t} \int_{z_1}^{z_2} C_x(z) dz \quad (4)$$

Here,  $L_x$  ( $P_x$ ) is the loss (production) rate of species  $x$  happening within the time window of turbulent air movement from within the canopy (height  $z_1$ ) to above the canopy

(height  $z_2$ ). We choose 4.4 m, averaged throughout the canopy, as a representative of  $z_1$  and 18 m above canopy layer as representative of  $z_2$ .

PNs can act as either a net source or a sink of  $\text{NO}_x$  through thermal dissociation (+1  $\text{NO}_2$  molecule) or PN formation (-1  $\text{NO}_2$ ). Calculating the steady-state chemical production and thermal and chemical loss of PAN (LaFranchi et al., 2009; Wolfe et al., 2009), yields 5.3 ppt of  $\text{NO}_2$  formed in 100 s. This mechanism implies an enhancement of  $\text{NO}_x$  within the canopy, as discussed in more detail in Min et al., (2013). However, we have also suggested that a local biogenic precursor drives PN formation within canopy (Min et al., 2012). This BVOC PN species, denoted XPN, exhibited an upward flux and is a candidate for  $\text{NO}_2$  loss not included in our steady-state calculation. We estimate the flux of this XPN to be  $2.3 \pm 0.4 \text{ ppt ms}^{-1}$  corresponding to 16.7 ppt of  $\text{NO}_2$  loss within canopy and explaining 31 % of the  $\text{NO}_x C_{\text{DELTA}}$ .

BVOC driven AN formation from OH initiated chemistry can be calculated as:

$$P_{\Sigma \text{AN}} = \sum_i \gamma_i \alpha_i k_{\text{OH}+\text{VOC}_i} [\text{OH}] [\text{VOC}_i] \quad (5)$$

where

$$\gamma_i = \frac{k_{\text{RO}_2 i + \text{NO}} [\text{NO}]}{k_{\text{RO}_2 i + \text{NO}} [\text{NO}] + k_{\text{RO}_2 i + \text{HO}_2} [\text{HO}_2] + \sum_j k_{\text{RO}_2 i + \text{RO}_2 j} [\text{RO}_2]_j + k_{\text{isom}}} \quad (6)$$

Here,  $\alpha_i$  and  $\gamma_i$  stands for branching ratio of AN formation from  $\text{RO}_2$  and NO reaction and the fraction of  $\text{RO}_2 i$  from  $\text{VOC}_i$  reacts with NO. Also,  $k_{\text{isom}}$  refers the unimolecular isomerization rate of  $\text{RO}_2 i$ . We estimate the effects of MBO, monoterpenes and isoprene, important BVOCs at the BEARPEX site (Bouvier-Brown et al., 2009; Schade et al., 2000), on AN production (for 100 s) and calculate 3.1 ppt (5.7 %), 0.4 ppt (0.7 %) and 6.9 ppt (12.8 %)  $\text{NO}_x$  is removed by AN formation, respectively. We use a 10, 11.7 and 18 % branching ratio ( $\alpha_i$ ) for MBO (Chan et al., 2009), isoprene (Paulot et al., 2009) and monoterpenes (Paulot et al., 2009). The rate constants and mechanisms for

12458

Observational  
evidence for within  
canopy removal of  
 $\text{NO}_x$

K.-E. Min et al.

Title Page

Abstract

Introduction

Conclusions

References

Tables

Figures

⏪

⏩

◀

▶

Back

Close

Full Screen / Esc

Printer-friendly Version

Interactive Discussion



## Observational evidence for within canopy removal of NO<sub>x</sub>

K.-E. Min et al.

Title Page

Abstract

Introduction

Conclusions

References

Tables

Figures

⏪

⏩

◀

▶

Back

Close

Full Screen / Esc

Printer-friendly Version

Interactive Discussion

RO<sub>2</sub> + HO<sub>2</sub>, RO<sub>2</sub> + NO and RO<sub>2</sub> + RO<sub>2</sub> were taken from the Master Chemical Mechanism (MCM) v3.2 (Jenkin et al., 1997; Saunders et al., 2003) and isomerization rates for isoprene from Crouse et al. (2011). If we consider AN formation from ozonolysis reactions of very reactive BVOCs, such as sesquiterpenes in analogy to XPN formation through the channel described as BCSOZNO<sub>3</sub> in MCM v3.2, we estimate additional 16.8 ppt (31.1 %) of NO<sub>x</sub> consumed. These calculations indicate chemical formation of nitrates is rapid enough to affect the fluxes.

Formation of HNO<sub>3</sub> is also a potentially important pathway for removal of NO<sub>x</sub> from the system by wet and dry deposition after formation. The gas phase reaction of NO<sub>2</sub> with OH is the major source of HNO<sub>3</sub> formation (heterogeneous formation HNO<sub>3</sub> from NO<sub>2</sub> hydrolysis is slower by an order of magnitude order than the gas phase formation rate), although hydrolysis of tertiary organic nitrates may also be important (Darer et al., 2011; Hu et al., 2011; Browne et al., 2013). The production rate can be calculated as:

$$P_{\text{HNO}_3} = k_{\text{OH}+\text{NO}_2}[\text{OH}][\text{NO}_2] \quad (7)$$

Using the measured OH concentration, we estimate 0.6–2 % of NO<sub>x</sub> is lost through gas phase reaction at this site. Compared to ANs and PNs, HNO<sub>3</sub> formation by OH reactions is unimportant.

HONO formation is another candidate for altering the flux of NO<sub>x</sub>. HONO flux measurements at this site were observed to be small ( $-0.11 \pm 0.69 \text{ ppt ms}^{-1}$ ) and slightly downward contributing to the enhancement of NO<sub>x</sub> within canopy rather than loss.

Direct uptake through plant stomata might be responsible for the remaining NO<sub>2</sub> removal within the canopy. We estimate < 2.5 ppt of NO<sub>2</sub> is removed through plant leaves at the typical daytime NO<sub>2</sub> concentration and canopy conductance (< 1 cm s<sup>-1</sup> with 3.7 m<sup>2</sup> m<sup>-2</sup>) assuming uptake rates similar to those reported in recent field and laboratory studies (Chapparro-Suarez et al., 2011; Breuninger et al., 2012, 2013). However, the daytime NO<sub>2</sub> concentration at this site of less than few hundred ppt suggests this site is a regime where NO<sub>2</sub> emissions from plant biota likely dominate, consistent with the result of Breuninger et al. (2013) who estimate 0.05–0.65 ppb as NO<sub>2</sub>

compensation point in a Norway Spruce forest. Further evidence for an NO<sub>2</sub> compensation point from canopy scale observations will be presented in Min et al. (2013).

Taken together as much as 86 % of the C<sub>DELTA</sub> for NO<sub>x</sub> (Table 2) can be explained by local chemical NO<sub>x</sub> loss mechanisms and the formation of higher nitrogen oxides.

5 Given the uncertainties, it is reasonable to interpret this as indicating all of the C<sub>DELTA</sub> is due to within canopy chemistry. This leads us to suggest a conceptual model for biosphere-atmosphere exchange of NO<sub>x</sub> as shown in Fig. 12. In addition to the previously suggested within canopy process of NO<sub>x</sub> (Fig. 1), chemical pathways are added  
10 converting NO<sub>x</sub> to higher oxides of N. These pathways are alternative mechanisms to plant uptake that have the effect of reducing the soil NO that escapes the forest canopy. The direction and magnitude of higher nitrogen oxides fluxes in this coupled mechanism then are the net resultant of upward (owing to formation within canopy) and downward (deposition from the atmosphere) fluxes of each classes.

## 6 Conclusions

15 During the BEARPEX 2009 field experiment, we observed upward fluxes of NO and NO<sub>2</sub> using eddy-covariance flux measurements, along with large NO<sub>2</sub> and NO<sub>x</sub> concentration enhancements within canopy, and counter-gradient fluxes of NO. Applying standard flux-gradient relationships to interpret the data indicates the existence of one or more NO<sub>x</sub> loss processes within the canopy, in addition to conversion of NO to NO<sub>2</sub>  
20 by reaction with O<sub>3</sub> and peroxy radicals. We interpret these results as observational evidence for an ecosystem scale canopy reduction factor, a factor that has been relied on to reconcile discordance between leaf-level, soil-level, and atmospheric modeling studies. We investigate multiple chemical and ecophysiological processes to explain the NO<sub>x</sub> removal during vertical transport and conclude that the chemical formation  
25 of PNs and ANs are the primary mechanisms responsible – implying that the reactive nitrogen does escape the canopy and may be returned by further chemistry as NO<sub>x</sub> downwind.

**Observational  
evidence for within  
canopy removal of  
NO<sub>x</sub>**

K.-E. Min et al.

Title Page

Abstract

Introduction

Conclusions

References

Tables

Figures

⏪

⏩

◀

▶

Back

Close

Full Screen / Esc

Printer-friendly Version

Interactive Discussion





*Acknowledgements.* This research was supported by the National Science Foundation (grants NSF-AGS 1120076 and ATM-0639847). We thank Sierra Pacific Industries for use of their land, and the University of California, Berkeley, Blodgett Forest Research Station for cooperation in facilitating this research. We also thank to Dennis D. Baldocchi for helpful comments on EC flux.

## References

- Anderson, I. C. and Poth, M. A.: Semiannual losses of nitrogen as NO and N<sub>2</sub>O from unburned and burned chaparral, *Global Biogeochem. Cy.*, 3, 121–135, 1989.
- Baldocchi, D. D., Hicks, B. B., and Meyers, T. P.: Measuring biosphere–atmosphere exchanges of biologically related gases with micrometeorological methods, *Ecology*, 69, 1331–1340, 1988.
- Bargsten, A., Falge, E., Pritsch, K., Huwe, B., and Meixner, F. X.: Laboratory measurements of nitric oxide release from forest soil with a thick organic layer under different understory types, *Biogeosciences*, 7, 1425–1441, doi:10.5194/bg-7-1425-2010, 2010.
- Bouvier-Brown, N. C., Goldstein, A. H., Gilman, J. B., Kuster, W. C., and de Gouw, J. A.: In-situ ambient quantification of monoterpenes, sesquiterpenes, and related oxygenated compounds during BEARPEX 2007: implications for gas- and particle-phase chemistry, *Atmos. Chem. Phys.*, 9, 5505–5518, doi:10.5194/acp-9-5505-2009, 2009a.
- Bouvier-Brown, N. C., Holzinger, R., Palitzsch, K., and Goldstein, A. H.: Large emissions of sesquiterpenes and methyl chavicol quantified from branch enclosure measurements, *Atmos. Environ.*, 43, 389–401, doi:10.1016/j.atmosenv.2008.08.039, 2009b.
- Breuninger, C., Oswald, R., Kesselmeier, J., and Meixner, F. X.: The dynamic chamber method: trace gas exchange fluxes (NO, NO<sub>2</sub>, O<sub>3</sub>) between plants and the atmosphere in the laboratory and in the field, *Atmos. Meas. Tech.*, 5, 955–989, doi:10.5194/amt-5-955-2012, 2012.
- Breuninger, C., Kesselmeier, J., and Meixner, F. X.: Field investigations of nitrogen dioxide (NO<sub>2</sub>) exchange between plants and the atmosphere, *Atmos. Chem. Phys.*, 13, 773–790, doi:10.5194/acp-13-773-2013, 2013.
- Browne, E. C., Min, K.-E., Wooldridge, P. J., Apel, E., Blake, D. R., Brune, W. H., Cantrell, C. A., Cubison, M. J., Diskin, G. S., Jimenez, J. L., Weinheimer, A. J., Wennberg, P. O., Wisthaler, A., and Cohen, R. C.: Observations of total RONO<sub>2</sub> over the boreal forest: NO<sub>x</sub>

Observational  
evidence for within  
canopy removal of  
NO<sub>x</sub>

K.-E. Min et al.

Title Page

Abstract

Introduction

Conclusions

References

Tables

Figures



Back

Close

Full Screen / Esc

Printer-friendly Version

Interactive Discussion

**Observational  
evidence for within  
canopy removal of  
NO<sub>x</sub>**

K.-E. Min et al.

Title Page

Abstract

Introduction

Conclusions

References

Tables

Figures

◀

▶

◀

▶

Back

Close

Full Screen / Esc

Printer-friendly Version

Interactive Discussion

sink and HNO<sub>3</sub> sources, *Atmos. Chem. Phys.*, 13, 4543–4562, doi:10.5194/acp-13-4543-2013, 2013.

Brummer, C., Marx, O., Kutsch, W., Ammann, C., Wolff, V., Flechard, C. R., and Freibauer, A.: Fluxes of total reactive atmospheric nitrogen (Sigma N-r) using eddy covariance above arable land, *Tellus B*, 65, 19770, doi:10.3402/tellusb.v65i0.19770, 2013.

Butterbach-Bahl, K., Breuer, L., Gasche, R., Willibald, G., and Papen, H.: Exchange of trace gases between soils and the atmosphere in Scots pine forest ecosystems of the northeastern German lowlands 1. Fluxes of N<sub>2</sub>O, NO/NO<sub>2</sub> and CH<sub>4</sub> at forest sites with different N-deposition, *Forest Ecol. Manag.*, 167, 123–134, 2002.

Chan, A. W. H., Galloway, M. M., Kwan, A. J., Chhabra, P. S., Keutsch, F. N., Wennberg, P. O., Flagan, R. C., and Seinfeld, J. H.: Photooxidation of 2-Methyl-3-Buten-2-ol (MBO) as a potential source of secondary organic aerosol, *Environ. Sci. Technol.*, 43, 4647–4652, doi:10.1021/es902789a, 2009.

Chaparro-Suarez, I. G., Meixner, F. X., and Kesselmeier, J.: Nitrogen dioxide (NO<sub>2</sub>) uptake by vegetation controlled by atmospheric concentrations and plant stomatal aperture, *Atmos. Environ.*, 45, 5742–5750, doi:10.1016/j.atmosenv.2011.07.021, 2011.

Chen, X. Y., Mulder, J., Wang, Y. H., Zhao, D. W., and Xiang, R. J.: Atmospheric deposition, mineralization and leaching of nitrogen in subtropical forested catchments, South China, *Environ. Geochem. Hlth.*, 26, 179–186, 2004.

Choi, W., Faloon, I. C., McKay, M., Goldstein, A. H., and Baker, B.: Estimating the atmospheric boundary layer height over sloped, forested terrain from surface spectral analysis during BEARPEX, *Atmos. Chem. Phys.*, 11, 6837–6853, doi:10.5194/acp-11-6837-2011, 2011.

Cleary, P. A., Wooldridge, P. J., and Cohen, R. C.: Laser-induced fluorescence detection of atmospheric NO<sub>2</sub> with a commercial diode laser and a supersonic expansion, *Appl. Optics*, 41, 6950–6956, 2002.

Crouse, J. D., Paulot, F., Kjaergaard, H. G., and Wennberg, P. O.: Peroxy radical isomerization in the oxidation of isoprene, *Phys. Chem. Chem. Phys.*, 13, 13607, doi:10.1039/c1cp21330j, 2011.

Crutzen, P.: A discussion of the chemistry of some minor constituents in the stratosphere and troposphere, *Pure Appl. Geophys.*, 106, 1385–1399, doi:10.1007/BF00881092, 1973.

Darer, A. I., Cole-Filipiak, N. C., O'Connor, A. E., and Elrod, M. J.: Formation and stability of atmospherically relevant isoprene-derived organosulfates and organonitrates, *Environ. Sci. Technol.*, 45, 1895–1902, doi:10.1021/Es103797z, 2011.

## Observational evidence for within canopy removal of NO<sub>x</sub>

K.-E. Min et al.

Title Page

Abstract

Introduction

Conclusions

References

Tables

Figures

⏪

⏩

◀

▶

Back

Close

Full Screen / Esc

Printer-friendly Version

Interactive Discussion

- Davidson, E. A., Matson, P. A., Vitousek, P. M., Riley, R., Dunkin, K., Garciamendez, G., and Maass, J. M.: Processes regulating soil emissions of NO and N<sub>2</sub>O in a seasonally dry tropical forest, *Ecology*, 74, 130–139, 1993.
- Day, D. A., Wooldridge, P. J., Dillon, M. B., Thornton, J. A., and Cohen, R. C.: A thermal dissociation laser-induced fluorescence instrument for in situ detection of NO<sub>2</sub>, peroxy nitrates, alkyl nitrates, and HNO<sub>3</sub>, *J. Geophys. Res.*, 107, ACH4-1–ACH4-14, doi:10.1029/2001jd000779, 2002.
- Day, D. A., Dillon, M. B., Wooldridge, P. J., Thornton, J. A., Rosen, R. S., Wood, E. C., and Cohen, R. C.: On alkyl nitrates, O<sub>3</sub>, and the “missing NO<sub>y</sub>”, *J. Geophys. Res.-Atmos.*, 108, 4501, doi:10.1029/2003jd003685, 2003.
- Dillon, M. B., Lamanna, M. S., Schade, G. W., Goldstein, A. H., and Cohen, R. C.: Chemical evolution of the Sacramento urban plume: transport and oxidation, *J. Geophys. Res.-Atmos.*, 107, 4045, doi:10.1029/2001jd000969, 2002.
- Drummond, J. W., Volz, A., and Ehhalt, D. H.: An optimized chemi-luminescence detector for tropospheric no measurements, *J. Atmos. Chem.*, 2, 287–306, 1985.
- Farmer, D. K., Wooldridge, P. J., and Cohen, R. C.: Application of thermal-dissociation laser induced fluorescence (TD-LIF) to measurement of HNO<sub>3</sub>, Σalkyl nitrates, Σperoxy nitrates, and NO<sub>2</sub> fluxes using eddy covariance, *Atmos. Chem. Phys.*, 6, 3471–3486, doi:10.5194/acp-6-3471-2006, 2006.
- Feig, G. T., Mamtimin, B., and Meixner, F. X.: Soil biogenic emissions of nitric oxide from a semi-arid savanna in South Africa, *Biogeosciences*, 5, 1723–1738, doi:10.5194/bg-5-1723-2008, 2008.
- Foken, T.: *Micrometeorology*, Springer-Verlag, Berlin, Heidelberg, Germany, 2006.
- Foken, T. and Wichura, B.: Tools for quality assessment of surface-based flux measurements, *Agr. Forest Meteorol.*, 78, 83–105, 1996.
- Galloway, J. N., Dentener, F. J., Capone, D. G., Boyer, E. W., Howarth, R. W., Seitzinger, S. P., Asner, G. P., Cleveland, C. C., Green, P. A., Holland, E. A., Karl, D. M., Michaels, A. F., Porter, J. H., Townsend, A. R., and Vorosmarty, C. J.: Nitrogen cycles: past, present, and future, *Biogeochemistry*, 70, 153–226, 2004.
- Gao, W., Wesely, M. L., and Lee, I. Y.: A numerical study of the effects of air chemistry on fluxes of NO, NO<sub>2</sub>, and O<sub>3</sub> near the surface, *J. Geophys. Res.-Atmos.*, 96, 18761–18769, 1991.
- Gasche, R. and Papen, H.: Spatial variability of NO and NO<sub>2</sub> flux rates from soil of spruce and beech forest ecosystems, *Plant Soil*, 240, 67–76, 2002.

**Observational  
evidence for within  
canopy removal of  
NO<sub>x</sub>**

K.-E. Min et al.

Title Page

Abstract

Introduction

Conclusions

References

Tables

Figures

◀

▶

◀

▶

Back

Close

Full Screen / Esc

Printer-friendly Version

Interactive Discussion

Gbondo-Tugbawa, S. S. and Driscoll, C. T.: Evaluation of the effects of future controls on sulfur dioxide and nitrogen oxide emissions on the acid-base status of a northern forest ecosystem, *Atmos. Environ.*, 36, 1631–1643, 2002.

5 Gut, A., Scheibe, M., Rottenberger, S., Rummel, U., Welling, M., Ammann, C., Kirkman, G. A., Kuhn, U., Meixner, F. X., Kesselmeier, J., Lehmann, B. E., Schmidt, W., Muller, E., and Piedade, M. T. F.: Exchange fluxes of NO<sub>2</sub> and O<sub>3</sub> at soil and leaf surfaces in an Amazonian rain forest, *J. Geophys. Res.-Atmos.*, 107, 8060, doi:10.1029/2001jd000654, 2002a.

10 Gut, A., van Dijk, S. M., Scheibe, M., Rummel, U., Welling, M., Ammann, C., Meixner, F. X., Kirkman, G. A., Andreae, M. O., and Lehmann, B. E.: NO emission from an Amazonian rain forest soil: continuous measurements of NO flux and soil concentration, *J. Geophys. Res.-Atmos.*, 107, 8057, doi:10.1029/2001jd000521, 2002b.

Hereid, D. P. and Monson, R. K.: Nitrogen oxide fluxes between corn (*Zea mays* L.) leaves and the atmosphere, *Atmos. Environ.*, 35, 975–983, 2001.

15 Herman, D. J., Halverson, L. J., and Firestone, M. K.: Nitrogen dynamics in an annual grassland: oak canopy, climate, and microbial population effects, *Ecol. Appl.*, 13, 593–604, 2003.

Herman, F., Smidt, S., Huber, S., Englisch, M., and Knoflacher, M.: Evaluation of pollution-related stress factors for forest ecosystems in central Europe, *Environ. Sci. Pollut. R.*, 8, 231–242, 2001.

20 Hessen, D. O., Henriksen, A., Hindar, A., Mulder, J., Torseth, K., and Vagstad, N.: Human impacts on the nitrogen cycle: a global problem judged from a local perspective, *Ambio*, 26, 321–325, 1997.

Hietz, P., Turner, B. L., Wanek, W., Richter, A., Nock, C. A., and Wright, S. J.: Long-term change in the nitrogen cycle of tropical forests, *Science*, 334, 664–666, doi:10.1126/science.1211979, 2011.

25 Holland, E. A. and Lamarque, J. F.: Modeling bio-atmospheric coupling of the nitrogen cycle through NO<sub>x</sub> emissions and NO<sub>y</sub> deposition, *Nutr. Cycl. Agroecosys.*, 48, 7–24, 1997.

Holland, E. A., Braswell, B. H., Lamarque, J. F., Townsend, A., Sulzman, J., Muller, J. F., Dentener, F., Brasseur, G., Levy, H., Penner, J. E., and Roelofs, G. J.: Variations in the predicted spatial distribution of atmospheric nitrogen deposition and their impact on carbon uptake by terrestrial ecosystems, *J. Geophys. Res.-Atmos.*, 102, 15849–15866, 1997.

30 Holzinger, R., Lee, A., Paw, K. T., and Goldstein, U. A. H.: Observations of oxidation products above a forest imply biogenic emissions of very reactive compounds, *Atmos. Chem. Phys.*, 5, 67–75, doi:10.5194/acp-5-67-2005, 2005.

## Observational evidence for within canopy removal of NO<sub>x</sub>

K.-E. Min et al.

Title Page

Abstract

Introduction

Conclusions

References

Tables

Figures

◀

▶

◀

▶

Back

Close

Full Screen / Esc

Printer-friendly Version

Interactive Discussion

- Horii, C. V.: Tropospheric reactive nitrogen speciation, deposition and chemistry at Harvard Forest, Ph.D., Harvard University, Cambridge, MA, USA, 2002.
- Horii, C. V., Munger, J. W., Wofsy, S. C., Zahniser, M., Nelson, D., and McManus, J. B.: Fluxes of nitrogen oxides over a temperate deciduous forest, *J. Geophys. Res.-Atmos.*, 109, D08305, doi:10.1029/2003jd004326, 2004.
- Hu, K. S., Darer, A. I., and Elrod, M. J.: Thermodynamics and kinetics of the hydrolysis of atmospherically relevant organonitrates and organosulfates, *Atmos. Chem. Phys.*, 11, 8307–8320, doi:10.5194/acp-11-8307-2011, 2011.
- Hungate, B. A., Dukes, J. S., Shaw, M. R., Luo, Y. Q., and Field, C. B.: Nitrogen and climate change, *Science*, 302, 1512–1513, 2003.
- Jacob, D. J. and Wofsy, S. C.: Budgets of Reactive Nitrogen, Hydrocarbons, and Ozone over the Amazon-Forest during the Wet Season, *J. Geophys. Res.-Atmos.*, 95, 16737–16754, 1990.
- Jenkin, M. E., Saunders, S. M., and Pilling, M. J.: The tropospheric degradation of volatile organic compounds: a protocol for mechanism development, *Atmos. Environ.*, 31, 81–104, doi:10.1016/S1352-2310(96)00105-7, 1997.
- Kaimal, J. C. and Finnigan, J. J.: *Atmospheric Boundary Layer Flows: their Structure and Measurement*, Oxford University Press, New York, NY, USA, 1994.
- Karl, T., Harley, P., Guenther, A., Rasmussen, R., Baker, B., Jardine, K., and Nemitz, E.: The bidirectional exchange of oxygenated VOCs between a loblolly pine (*Pinus taeda*) plantation and the atmosphere, *Atmos. Chem. Phys.*, 5, 3015–3031, doi:10.5194/acp-5-3015-2005, 2005.
- Kurpius, M. R. and Goldstein, A. H.: Gas-phase chemistry dominates O<sub>3</sub> loss to a forest, implying a source of aerosols and hydroxyl radicals to the atmosphere, *Geophys. Res. Lett.*, 30, 1371, doi:10.1029/2002gl016785, 2003.
- LaFranchi, B. W., Wolfe, G. M., Thornton, J. A., Harrold, S. A., Browne, E. C., Min, K. E., Wooldridge, P. J., Gilman, J. B., Kuster, W. C., Goldan, P. D., de Gouw, J. A., McKay, M., Goldstein, A. H., Ren, X., Mao, J., and Cohen, R. C.: Closing the peroxy acetyl nitrate budget: observations of acyl peroxy nitrates (PAN, PPN, and MPAN) during BEARPEX 2007, *Atmos. Chem. Phys.*, 9, 7623–7641, doi:10.5194/acp-9-7623-2009, 2009.
- LaFranchi, B. W., Goldstein, A. H., and Cohen, R. C.: Observations of the temperature dependent response of ozone to NO<sub>x</sub> reductions in the Sacramento, CA urban plume, *Atmos. Chem. Phys.*, 11, 6945–6960, doi:10.5194/acp-11-6945-2011, 2011.

## Observational evidence for within canopy removal of NO<sub>x</sub>

K.-E. Min et al.

Title Page

Abstract

Introduction

Conclusions

References

Tables

Figures

◀

▶

◀

▶

Back

Close

Full Screen / Esc

Printer-friendly Version

Interactive Discussion



Lee, X., Massman, W., and Law, B.: Handbook of Micrometeorology: a Guide for Surface Flux Measurement and Analysis, Kluwer Academic Publishers, Dordrecht, the Netherlands, 2004.

Lerdau, M. T., Munger, L. J., and Jacob, D. J.: Atmospheric chemistry – the NO<sub>2</sub> flux conundrum, *Science*, 289, 2291–2293, doi:10.1126/science.289.5488.2291, 2000.

Li, D. J. and Wang, X. M.: Nitric oxide emission following wetting of dry soils in subtropical humid forests, *Pedosphere*, 19, 692–699, doi:10.1016/S1002-0160(09)60164-8, 2009.

Lockwood, A. L., Filley, T. R., Rhodes, D., and Shepson, P. B.: Foliar uptake of atmospheric organic nitrates, *Geophys. Res. Lett.*, 35, L15809, doi:10.1029/2008gl034714, 2008.

Makarov, M. I. and Kiseleva, V. V.: Acidification and nutrient imbalance in forest soils subjected to nitrogen deposition, *Water Air Soil Poll.*, 85, 1137–1142, 1995.

Massman, W. J.: The attenuation of concentration fluctuations in turbulent-flow through a tube, *J. Geophys. Res.-Atmos.*, 96, 15269–15273, 1991.

Mayer, J. C., Bargsten, A., Rummel, U., Meixner, F. X., and Foken, T.: Distributed Modified Bowen Ratio method for surface layer fluxes of reactive and non-reactive trace gases, *Agr. Forest Meteorol.*, 151, 655–668, doi:10.1016/j.agrformet.2010.10.001, 2011.

McMillen, R. T.: An Eddy-correlation technique with extended applicability to non-simple terrain, *Bound.-Lay. Meteorol.*, 43, 231–245, 1988.

Meyer, K.: Effects of fuel-element vibrations on spectral density of neutron-flux fluctuations in pressurized water-reactors, *Kernenergie*, 29, 49–50, 1986.

Min, K.-E., Pusede, S. E., Browne, E. C., LaFranchi, B. W., Wooldridge, P. J., Wolfe, G. M., Harrold, S. A., Thornton, J. A., and Cohen, R. C.: Observations of atmosphere-biosphere exchange of total and speciated peroxy nitrates: nitrogen fluxes and biogenic sources of peroxy nitrates, *Atmos. Chem. Phys.*, 12, 9763–9773, doi:10.5194/acp-12-9763-2012, 2012.

Min, K.-E., Pusede, S. E., Browne, E. C., LaFranchi, B. W., Wooldridge, P. J., and Cohen, R. C.: Observational evidence for an ecosystem scale NO<sub>2</sub> compensation point, *Atmos. Chem. Phys. Discuss.*, in preparation, 2013.

Moore, C. J.: Frequency-response corrections for Eddy-correlation systems, *Bound.-Lay. Meteorol.*, 37, 17–35, 1986.

Morikawa, H., Takahashi, M., Sakamoto, A., Matsubara, T., Arimura, G. I., Kawamura, Y., Fukunaga, K., Fujita, K., Sakurai, N., Hirata, T., Ide, H., Nonoyama, N., and Suzuki, H.: Formation of unidentified nitrogen in plants: an implication for a novel nitrogen metabolism, *Planta*, 219, 14–22, doi:10.1007/s00425-003-1200-7, 2004a.

**Observational  
evidence for within  
canopy removal of  
NO<sub>x</sub>**

K.-E. Min et al.

Title Page

Abstract

Introduction

Conclusions

References

Tables

Figures

◀

▶

◀

▶

Back

Close

Full Screen / Esc

Printer-friendly Version

Interactive Discussion

Morikawa, T., Oikawa, A., Wadano, A., Yano, K., Sakurai, N., Suzuki, H., Saito, K., Shibata, D., and Ohta, D.: Plant metabolomic analyses by FT-ICR/MS, GC/MS, and LC/MS, *Plant Cell Physiol.*, 45, 206–S206, 2004b.

Neiryneck, J., Kowalski, A. S., Carrara, A., Genouw, G., Berghmans, P., and Ceulemans, R.: Fluxes of oxidised and reduced nitrogen above a mixed coniferous forest exposed to various nitrogen emission sources, *Environ. Pollut.*, 149, 31–43, 2007.

Norby, R. J., Warren, J. M., Iversen, C. M., Medlyn, B. E., and McMurtrie, R. E.: CO<sub>2</sub> enhancement of forest productivity constrained by limited nitrogen availability, *P. Natl. Acad. Sci. USA*, 107, 19368–19373, doi:10.1073/pnas.1006463107, 2010.

Oka, E., Tagami, Y., Oohashi, T., and Kondo, N.: A physiological and morphological study on the injury caused by exposure to the air pollutant, peroxyacetyl nitrate (PAN), based on the quantitative assessment of the injury, *J. Plant. Res.*, 117, 27–36, doi:10.1007/s10265-003-0127-1, 2004.

Ollinger, S. V., Aber, J. D., Reich, P. B., and Freuder, R. J.: Interactive effects of nitrogen deposition, tropospheric ozone, elevated CO<sub>2</sub> and land use history on the carbon dynamics of northern hardwood forests, *Global Change Biol.*, 8, 545–562, 2002a.

Ollinger, S. V., Smith, M. L., Martin, M. E., Hallett, R. A., Goodale, C. L., and Aber, J. D.: Regional variation in foliar chemistry and N cycling among forests of diverse history and composition, *Ecology*, 83, 339–355, 2002b.

Ordin, L., Garber, M. J., Kindinge, Ji, Whitmore, S. A., Greve, L. C., and Taylor, O. C.: Effect of peroxyacetyl nitrate (PAN) in-vivo on tobacco leaf polysaccharide synthetic pathways enzymes, *Environ. Sci. Technol.*, 5, 621–626, 1971.

Park, J.-H., Fares, S., Weber, R., and Goldstein, A. H.: Biogenic volatile organic compound emissions during BEARPEX 2009 measured by eddy covariance and flux-gradient similarity methods, *Atmos. Chem. Phys. Discuss.*, 12, 25081–25120, doi:10.5194/acpd-12-25081-2012, 2012.

Park, J.-H., Goldstein, A. H., Timkovsky, J., Fares, S., Weber, R., Karlik, J., and Holzinger, R.: Observations demonstrate active atmosphere-biosphere exchange of the vast majority of VOC, *Science*, in review, 2013.

Paulot, F., Crouse, J. D., Kjaergaard, H. G., Kroll, J. H., Seinfeld, J. H., and Wennberg, P. O.: Isoprene photooxidation: new insights into the production of acids and organic nitrates, *Atmos. Chem. Phys.*, 9, 1479–1501, doi:10.5194/acp-9-1479-2009, 2009.





## Observational evidence for within canopy removal of NO<sub>x</sub>

K.-E. Min et al.

Title Page

Abstract

Introduction

Conclusions

References

Tables

Figures

⏪

⏩

◀

▶

Back

Close

Full Screen / Esc

Printer-friendly Version

Interactive Discussion



Sparks, J. P., Monson, R. K., Sparks, K. L., and Lerdau, M.: Leaf uptake of nitrogen dioxide (NO<sub>2</sub>) in a tropical wet forest: implications for tropospheric chemistry, *Oecologia*, 127, 214–221, 2001.

Sparks, J. P.: Ecological ramifications of the direct foliar uptake of nitrogen, *Oecologia*, 159, 1–13, doi:10.1007/s00442-008-1188-6, 2009.

Takahashi, M., Nakagawa, M., Sakamoto, A., Ohsumi, C., Matsubara, T., and Morikawa, H.: Atmospheric nitrogen dioxide gas is a plant vitalization signal to increase plant size and the contents of cell constituents, *New Phytol.*, 168, 149–153, doi:10.1111/j.1469-8137.2005.01493.x, 2005a.

Takahashi, M., Nakayama, N., and Arihara, J.: Plant nitrogen levels and photosynthesis in the supernodulating soybean (*Glycine max* L. Merr.) cultivar “Sakukei 4”, *Plant Prod. Sci.*, 8, 412–418, 2005b.

Teklemariam, T. A. and Sparks, J. P.: Gaseous fluxes of peroxyacetyl nitrate (PAN) into plant leaves, *Plant Cell Environ.*, 27, 1149–1158, 2004.

Thornton, J. A., Wooldridge, P. J., and Cohen, R. C.: Atmospheric NO<sub>2</sub>: in situ laser-induced fluorescence detection at parts per trillion mixing ratios, *Anal. Chem.*, 72, 528–539, 2000.

Townsend, A. R., Braswell, B. H., Holland, E. A., and Penner, J. E.: Spatial and temporal patterns in terrestrial carbon storage due to deposition of fossil fuel nitrogen, *Ecol. Appl.*, 6, 806–814, 1996.

Turnipseed, A. A., Huey, L. G., Nemitz, E., Stickel, R., Higgs, J., Tanner, D. J., Slusher, D. L., Sparks, J. P., Flocke, F., and Guenther, A.: Eddy covariance fluxes of peroxyacetyl nitrates (PANs) and NO(y) to a coniferous forest, *J. Geophys. Res.-Atmos.*, 111, D09304, doi:10.1029/2005jd006631, 2006.

van Dijk, S. M., Gut, A., Kirkman, G. A., Meixner, F. X., Andreae, M. O., and Gomes, B. M.: Biogenic NO emissions from forest and pasture soils: relating laboratory studies to field measurements, *J. Geophys. Res.-Atmos.*, 107, 8058, doi:10.1029/2001jd000358, 2002.

Vandenhurk, B. J. J. M. and Mcnaughton, K. G.: Implementation of near-field dispersion in a simple 2-layer surface-resistance model, *J. Hydrol.*, 166, 293–311, 1995.

Vila-Guerau de Arellano, J., Duynkerke, P. G., and Bultjes, P. J. H.: The divergence of the turbulent-diffusion flux in the surface-layer due to chemical-reactions – the NO-O<sub>3</sub>-NO<sub>2</sub> system, *Tellus B*, 45, 23–33, 1993.

Vitousek, P. M. and Farrington, H.: Nutrient limitation and soil development: experimental test of a biogeochemical theory, *Biogeochemistry*, 37, 63–75, 1997.

## Observational evidence for within canopy removal of NO<sub>x</sub>

K.-E. Min et al.

Title Page

Abstract

Introduction

Conclusions

References

Tables

Figures

⏪

⏩

◀

▶

Back

Close

Full Screen / Esc

Printer-friendly Version

Interactive Discussion

Wang, Y. P. and Leuning, R.: A two-leaf model for canopy conductance, photosynthesis and partitioning of available energy I: model description and comparison with a multi-layered model, *Agr. Forest Meteorol.*, 91, 89–111, 1998.

Wesely, M. L., Eastman, J. A., Stedman, D. H., and Yalvac, E. D.: An Eddy-correlation measurement of NO<sub>2</sub> flux to vegetation and comparison to O<sub>3</sub> flux, *Atmos. Environ.*, 16, 815–820, 1982.

Wildt, J., Kley, D., Rockel, A., Rockel, P., and Segschneider, H. J.: Emission of NO from several higher plant species, *J. Geophys. Res.-Atmos.*, 102, 5919–5927, 1997.

Wolfe, G. M., Thornton, J. A., Yataavelli, R. L. N., McKay, M., Goldstein, A. H., LaFranchi, B., Min, K.-E., and Cohen, R. C.: Eddy covariance fluxes of acyl peroxy nitrates (PAN, PPN and MPAN) above a Ponderosa pine forest, *Atmos. Chem. Phys.*, 9, 615–634, doi:10.5194/acp-9-615-2009, 2009.

Wolfe, G. M., Thornton, J. A., Bouvier-Brown, N. C., Goldstein, A. H., Park, J.-H., McKay, M., Matross, D. M., Mao, J., Brune, W. H., LaFranchi, B. W., Browne, E. C., Min, K.-E., Wooldridge, P. J., Cohen, R. C., Crouse, J. D., Faloona, I. C., Gilman, J. B., Kuster, W. C., de Gouw, J. A., Huisman, A., and Keutsch, F. N.: The Chemistry of Atmosphere-Forest Exchange (CAFE) Model – Part 2: Application to BEARPEX-2007 observations, *Atmos. Chem. Phys.*, 11, 1269–1294, doi:10.5194/acp-11-1269-2011, 2011.

Yienger, J. J. and Levy, H.: Empirical-model of global soil-biogenic NO<sub>x</sub> emissions, *J. Geophys. Res.-Atmos.*, 100, 11447–11464, 1995.

Yu, J. B., Meixner, F. X., Sun, W. D., Mamtimin, B., Xia, C. H., and Xie, W. J.: Biogenic nitric oxide emission of mountain soils sampled from different vertical landscape zones in the Changbai Mountains, Northeastern China, *Environ. Sci. Technol.*, 44, 4122–4128, doi:10.1021/Es100380m, 2010.

Zapletal, M., Chroust, P., and Kunak, D.: The relationship between defoliation of Norway spruce and atmospheric deposition of sulphur and nitrogen compounds in the Hruby Jeseník Mts (the Czech Republic), *Ekol. Bratislava*, 22, 337–347, 2003.

## Observational evidence for within canopy removal of $\text{NO}_x$

K.-E. Min et al.

[Title Page](#)
[Abstract](#)
[Introduction](#)
[Conclusions](#)
[References](#)
[Tables](#)
[Figures](#)
[⏪](#)
[⏩](#)
[◀](#)
[▶](#)
[Back](#)
[Close](#)
[Full Screen / Esc](#)
[Printer-friendly Version](#)
[Interactive Discussion](#)


**Table 1.** Estimated flux analysis errors.

| Source of Error  | $F_{\text{NO}}$                            | $F_{\text{NO}_2}$       | $F_{\text{NO}_x}$       |                         |
|------------------|--|-------------------------|-------------------------|-------------------------|
| Systematic Error | Data acquisition scheme                    | < 2% (unbiased)         | < 3% (unbiased)         | < 4% (unbiased)         |
|                  | Sensor separation & High frequency damping | < 2% (underestimated)   | < 2% (underestimated)   | < 3% (underestimated)   |
|                  | Instrumental time                          | < 0.2% (underestimated) | < 0.7% (underestimated) | < 0.7% (underestimated) |
|                  | Absolute concentration estimation          | < 7% (unbiased)         | < 5% (unbiased)         | < 9% (unbiased)         |
|                  | Total                                      | < 8%                    | < 6%                    | < 10%                   |
| Random Error     | Instrument noise <sup>a</sup>              | < 20% (unbiased)        | < 10% (unbiased)        | < 23% (unbiased)        |
|                  | Detection limit concept <sup>b</sup>       | < 25% (unbiased)        | < 21% (unbiased)        | < 33% (unbiased)        |

<sup>a</sup> Errors over half an hour.

<sup>b</sup> Estimated from the ratio of covariances at true lag and several lag times far from the true lag ( $\pm 230$ – $250$  s).

## Observational evidence for within canopy removal of NO<sub>x</sub>

K.-E. Min et al.

**Table 2.** Possible within canopy NO<sub>x</sub> consumption mechanisms.

| Mechanisms                   | NO <sub>x</sub> consumption |               |
|------------------------------|-----------------------------|---------------|
|                              | [%]                         | [ppt]         |
| Un-identified PN formation   | 30.8 %                      | 16.7 ppt      |
| MBO and monoterpene nitrates | 19.2 %                      | 10.4 ppt      |
| Sesquiterpene nitrate        | 0–30.9 %                    | 0–16.8 ppt    |
| HNO <sub>3</sub>             | 0.6–2.0 %                   | 0.3–1.1 ppt   |
| HONO*                        | < –1.8 %                    | < –1.0 ppt    |
| Plant uptake                 | < 4.6 %                     | < 2.5 ppt     |
| Total NO <sub>x</sub> loss   | 53.4–85.7 %                 | 28.9–46.5 ppt |

\* Negative consumption indicates a source of NO<sub>x</sub> within the canopy.

Title Page

Abstract

Introduction

Conclusions

References

Tables

Figures

⏪

⏩

◀

▶

Back

Close

Full Screen / Esc

Printer-friendly Version

Interactive Discussion



## Observational evidence for within canopy removal of $\text{NO}_x$

K.-E. Min et al.

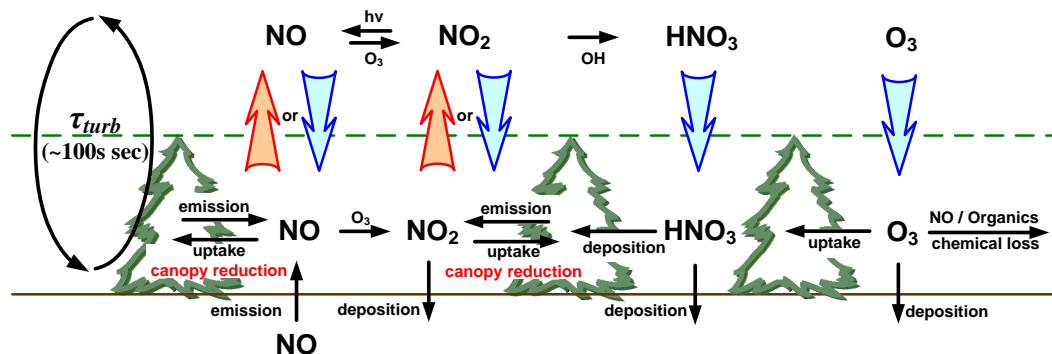


**Fig. 1.** Schematic of the various interactions involved in the exchange of nitrogen oxides between the atmosphere and the forest canopy. Bold arrows in blue (downward) and red (upward) represent the direction of the flux of each species across the canopy surface.

[Title Page](#)
[Abstract](#)
[Introduction](#)
[Conclusions](#)
[References](#)
[Tables](#)
[Figures](#)
[Back](#)
[Close](#)
[Full Screen / Esc](#)
[Printer-friendly Version](#)
[Interactive Discussion](#)

## Observational evidence for within canopy removal of $\text{NO}_x$

K.-E. Min et al.

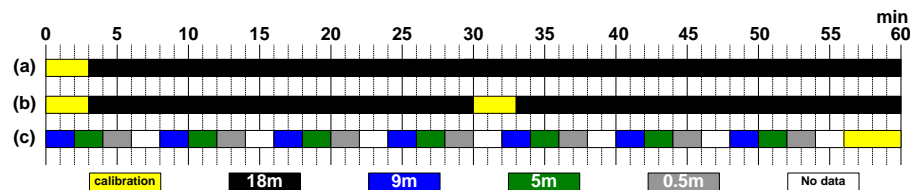


**Fig. 2.** Data collection scheme for fluxes of  $\text{NO}$  (**a**: 2ch-CL) and  $\text{NO}_2$  (**b**: TD-LIF) and vertical gradient (**c**) measurements. Colors represent the different measurement heights: 18 m (black), 9 m (blue), 5 m (green), and 0.5 m (gray). Yellow periods are calibration cycles and white periods represent times when diagnostics were collected.

Title Page

Abstract

Introduction

Conclusions

References

Tables

Figures

◀

▶

◀

▶

Back

Close

Full Screen / Esc

Printer-friendly Version

Interactive Discussion



**Observational  
evidence for within  
canopy removal of  
NO<sub>x</sub>**

K.-E. Min et al.

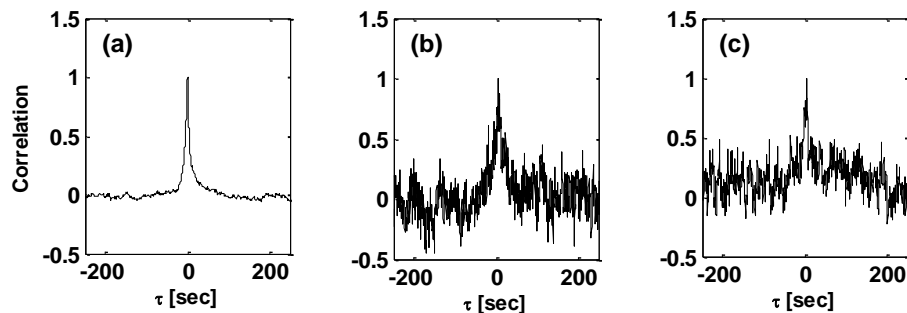


**Fig. 3.** Lag calculation of (a)  $w'T'$ , (b)  $w'NO'$  and (c)  $w'NO_2'$ . Highest normalized correlation between wind and temperature, NO or NO<sub>2</sub> were observed as expected; 0 s for wind and temperature, 1.4 and 2.6 s for NO and NO<sub>2</sub>.

[Title Page](#)[Abstract](#)[Introduction](#)[Conclusions](#)[References](#)[Tables](#)[Figures](#)[⏪](#)[⏩](#)[◀](#)[▶](#)[Back](#)[Close](#)[Full Screen / Esc](#)[Printer-friendly Version](#)[Interactive Discussion](#)

## Observational evidence for within canopy removal of $\text{NO}_x$

K.-E. Min et al.

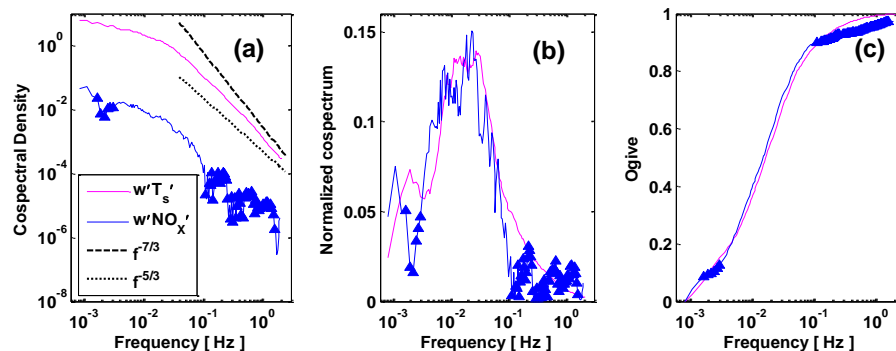


**Fig. 4.** Equally spaced logarithmic averaged (200 bins) absolute cospectral density **(a)**, frequency weighted cospectrum **(b)**, and normalized cumulative distributions of the cospectra of temperature (magenta) and  $\text{NO}_x$  (blue) **(c)** with vertical wind from 09:00–12:00 when the chemical perturbation is small. Closed triangles represent the absolute value of the negative cospectral density, which has the opposite sign to the general flux direction. The black dotted lines in **(a)** are lines with slopes of  $-7/3$  and  $-5/3$  (see related text).



## Observational evidence for within canopy removal of $\text{NO}_x$

K.-E. Min et al.

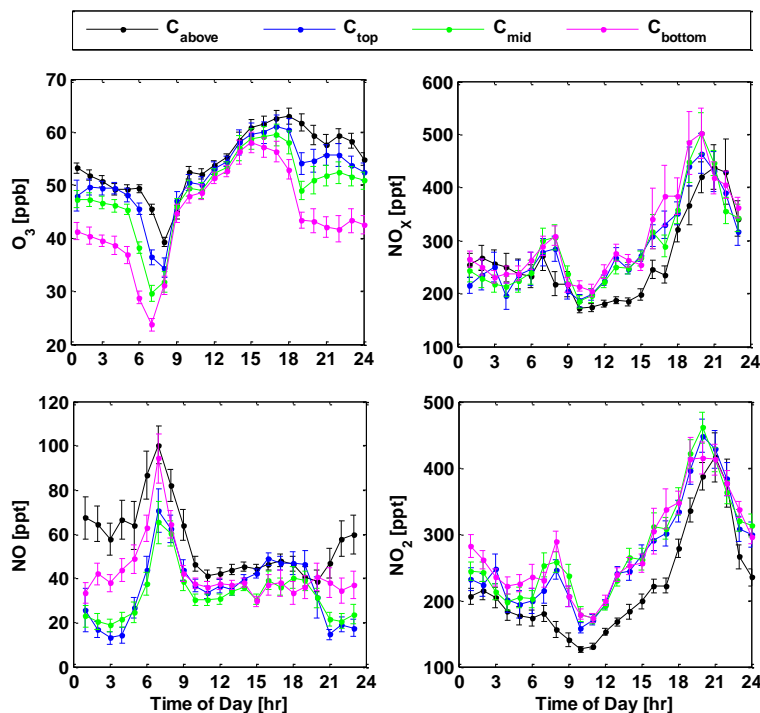


**Fig. 5.** Diurnal patterns of  $\text{O}_3$  (south tower),  $\text{NO}_x$ ,  $\text{NO}$ , and  $\text{NO}_2$ . The data are one-hour mean values and the error bars represent the variation defined as the observed variability ( $\pm 1\sigma$ ) divided by square root of the number of measurements in that time bin. Colors represent the measurement heights: above canopy (18 m) in black, top canopy (9 m) in blue, middle canopy (5 m) in green, and forest floor (1.5 m for  $\text{O}_3$  and 0.5 m for  $\text{NO}$  and  $\text{NO}_2$ ) in magenta.

[Title Page](#)
[Abstract](#)
[Introduction](#)
[Conclusions](#)
[References](#)
[Tables](#)
[Figures](#)
[◀](#)
[▶](#)
[◀](#)
[▶](#)
[Back](#)
[Close](#)
[Full Screen / Esc](#)
[Printer-friendly Version](#)
[Interactive Discussion](#)

## Observational evidence for within canopy removal of $\text{NO}_x$

K.-E. Min et al.

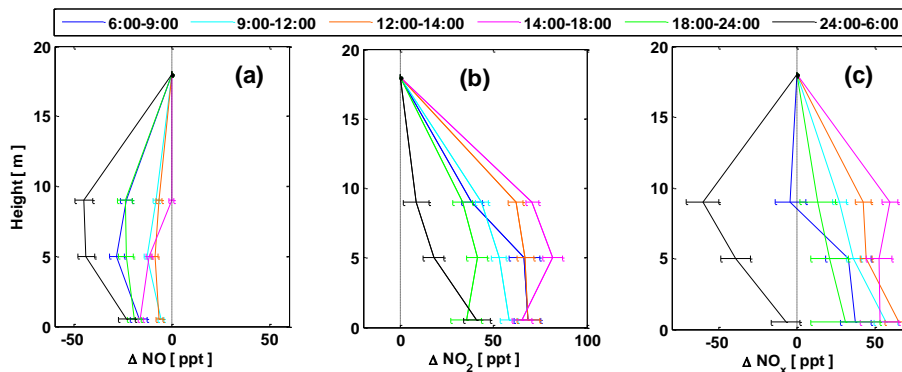


**Fig. 6.** Vertical gradients of  $\text{NO}$ ,  $\text{NO}_2$ , and  $\text{NO}_x$ . Dot and whiskers represent means and standard errors of the mixing ratio enhancement at each height. The colors represent the enhancement at 6 different times of day through the complete diurnal cycle: early morning (06:00–09:00, blue), late morning (09:00–12:00, cyan), midday (12:00–14:00, orange), afternoon (14:00–18:00, magenta), evening (18:00–24:00, green) and night (24:00–06:00, black).

Title Page

Abstract

Introduction

Conclusions

References

Tables

Figures

◀

▶

◀

▶

Back

Close

Full Screen / Esc

Printer-friendly Version

Interactive Discussion

## Observational evidence for within canopy removal of $\text{NO}_x$

K.-E. Min et al.

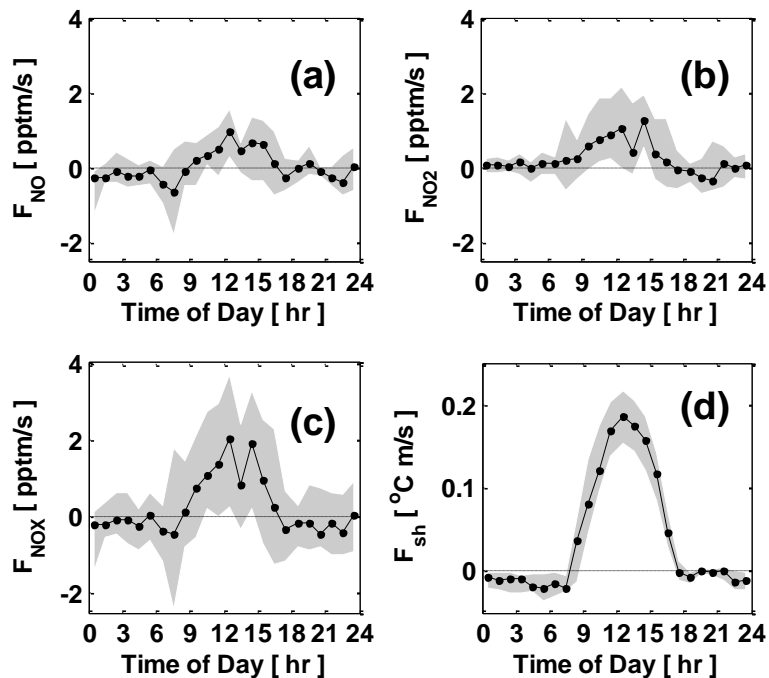


**Fig. 7.** Diurnal patterns of the  $\text{NO}$ ,  $\text{NO}_2$ ,  $\text{NO}_x$ , and sensible heat fluxes in panels (a–d), respectively. All fluxes are upward indicating molecular motion from forest to atmosphere. Median midday (12:00–14:00) fluxes are  $0.32 \pm 0.27$ ,  $0.67 \pm 0.21$ , and  $1.0 \pm 0.43$   $\text{pptm s}^{-1}$  for  $\text{NO}$ ,  $\text{NO}_2$ , and  $\text{NO}_x$  and that of sensible heat flux is  $0.21 \pm 0.08$   $^{\circ}\text{C m s}^{-1}$ . Black lines represent means and the gray areas give 25–75 % of flux data for hourly bins.

Title Page

Abstract

Introduction

Conclusions

References

Tables

Figures

◀

▶

◀

▶

Back

Close

Full Screen / Esc

Printer-friendly Version

Interactive Discussion

## Observational evidence for within canopy removal of $\text{NO}_x$

K.-E. Min et al.

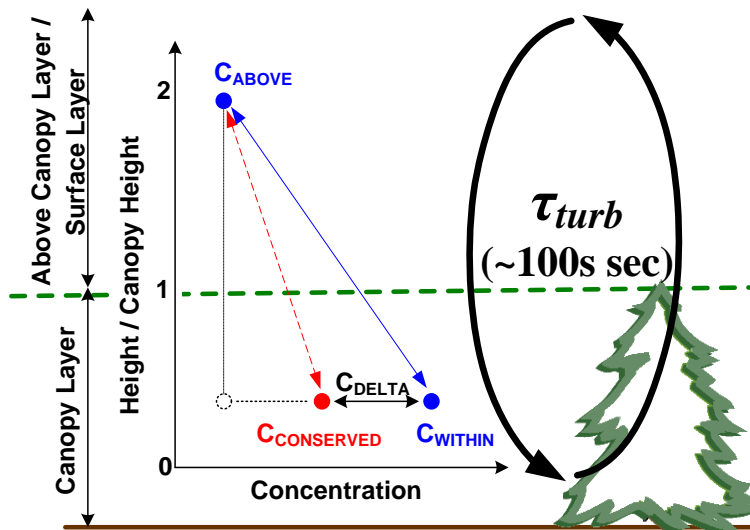


**Fig. 8.** Schematic of our two-layered model based on the localized-near field, LNF, concept.  $C_{\text{ABOVE}}$  represents the reference concentration, which for the above-canopy layer is defined as the measured concentration at height 18 m.  $C_{\text{WITHIN}}$  is the measured concentration within the canopy defined as the averaged concentration at 0.5, 5, and 9 m.  $C_{\text{CONSERVED}}$  is the estimated concentration based on the measured eddy-covariance flux and the eddy diffusivity calculated from sensible heat flux.  $C_{\text{DELTA}}$  is the difference between  $C_{\text{WITHIN}}$  and  $C_{\text{CONSERVED}}$  and is a measure of the importance of non-conservative processes.

[Title Page](#)
[Abstract](#)
[Introduction](#)
[Conclusions](#)
[References](#)
[Tables](#)
[Figures](#)
[Back](#)
[Close](#)
[Full Screen / Esc](#)
[Printer-friendly Version](#)
[Interactive Discussion](#)

## Observational evidence for within canopy removal of $\text{NO}_x$

K.-E. Min et al.

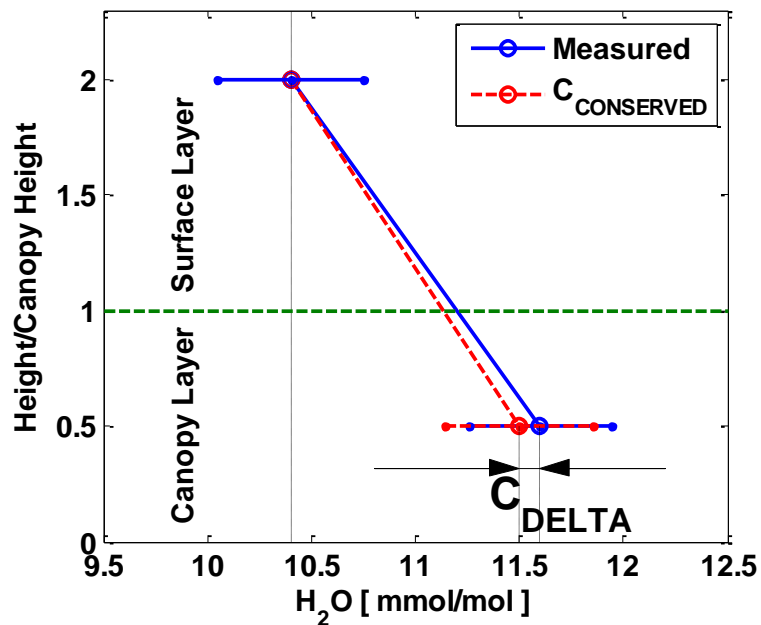


**Fig. 9.** The estimated concentration,  $C_{\text{CONSERVED}}$  (red) using standard flux-gradient similarities of  $\text{H}_2\text{O}$  during midday (12:00–14:00) is shown. Blue represents the measured vertical gradient. Open circles and whiskers represent the mean and the variability of  $\text{H}_2\text{O}$ . The difference between blue and red in the within-canopy level is shown in black arrow indicates  $C_{\text{DELTA}}$  and is negligibly small as expected for a conserved species.

## Observational evidence for within canopy removal of $\text{NO}_x$

K.-E. Min et al.

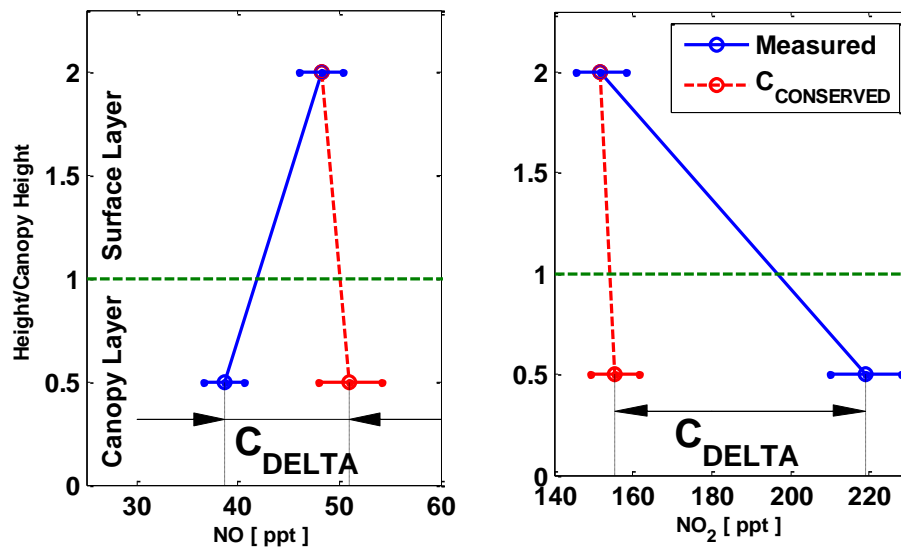


**Fig. 10.** The estimated concentration,  $C_{\text{CONSERVED}}$ , (red) using standard flux-gradient similarities of NO and  $\text{NO}_2$  at midday (12:00–14:00 and the measured vertical gradient (blue) giving values for  $C_{\text{DELTA}}$  of 12 ppt (NO) and 64 ppt ( $\text{NO}_2$ ).

Title Page

Abstract Introduction

Conclusions References

Tables Figures

⏪ ⏩

⏴ ⏵

Back Close

Full Screen / Esc

Printer-friendly Version

Interactive Discussion

Observational evidence for within canopy removal of  $\text{NO}_x$

K.-E. Min et al.

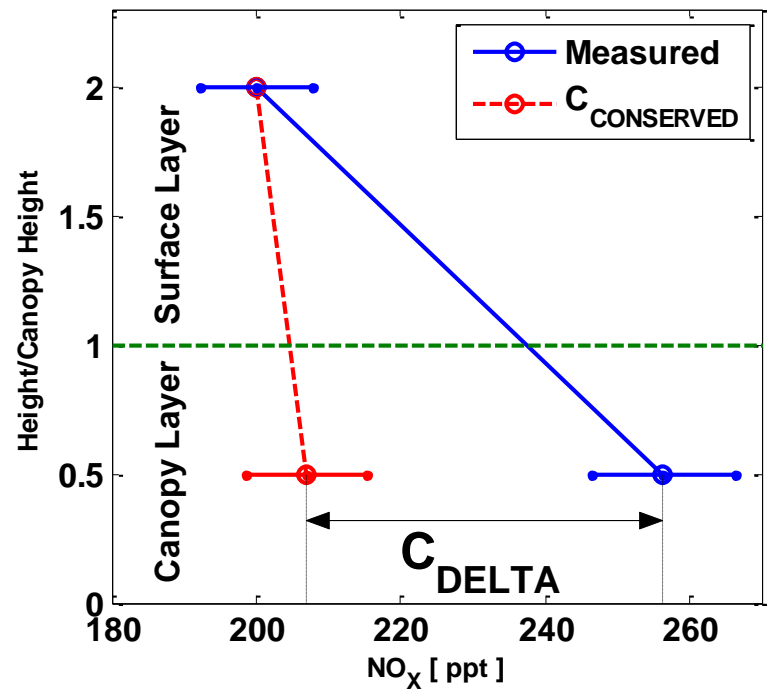


**Fig. 11.** The estimated concentration,  $C_{\text{CONSERVED}}$ , (red) using standard flux-gradient similarities of  $\text{NO}_x$  at midday (12:00–14:00) and the measured vertical gradient (blue) giving values for  $C_{\text{DELTA}}$  of  $\text{NO}_x$ . Open circles and whiskers are the mean and standard errors.

Title Page

Abstract

Introduction

Conclusions

References

Tables

Figures

◀

▶

◀

▶

Back

Close

Full Screen / Esc

Printer-friendly Version

Interactive Discussion



**Observational evidence for within canopy removal of  $\text{NO}_x$**

K.-E. Min et al.

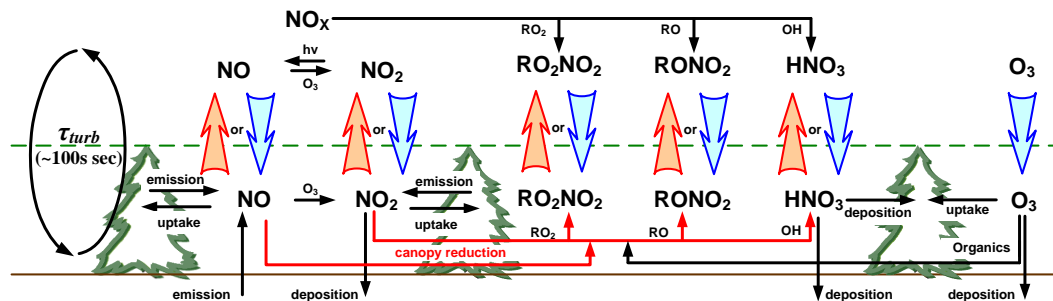


**Fig. 12.** Schematic of the interactions involved in the exchange of nitrogen oxides between the atmosphere and the forest canopy as identified in this manuscript. Bold arrows in blue (downward) and red (upward) represent the direction of the flux of each species across the canopy surface. Red thin arrows within canopy indicate the  $\text{NO}_x$  removal processes within the canopy in addition to plant uptake.

|                          |              |
|--------------------------|--------------|
| Title Page               |              |
| Abstract                 | Introduction |
| Conclusions              | References   |
| Tables                   | Figures      |
| ◀                        | ▶            |
| ◀                        | ▶            |
| Back                     | Close        |
| Full Screen / Esc        |              |
| Printer-friendly Version |              |
| Interactive Discussion   |              |